Mathematical Biosciences and Engineering

http://www.aimspress.com/journal/mbe

MBE, 19(10): 9792–9824.
DOI: 10.3934/mbe.2022456
Received: 20 May 2022
Revised: 16 June 2022
Accepted: 21 June 2022
Published: 08 July 2022

Research article

Modeling the effect of random diagnoses on the spread of COVID-19 in Saudi Arabia

Salma M. Al-Tuwairqi*and Sara K. Al-Harbi

Department of Mathematics, King Abdulaziz University, Jeddah, Saudi Arabia.

* **Correspondence:** Email: saltuwairqi@kau.edu.sa.

Abstract: Saudi Arabia was among the countries that attempted to manage the COVID-19 pandemic by developing strategies to control the epidemic. Lockdown, social distancing and random diagnostic tests are among these strategies. In this study, we formulated a mathematical model to investigate the impact of employing random diagnostic tests to detect asymptomatic COVID-19 patients. The model has been examined qualitatively and numerically. Two equilibrium points were obtained: the COVID-19 free equilibrium and the COVID-19 endemic equilibrium. The local and global asymptotic stability of the equilibrium points depends on the control reproduction number $\mathcal{R}_c$. The model was validated by employing the Saudi Ministry of Health COVID-19 dashboard data. Numerical simulations were conducted to substantiate the qualitative results. Further, sensitivity analysis was performed on $\mathcal{R}_c$ to scrutinize the significant parameters for combating COVID-19. Finally, different scenarios for implementing random diagnostic tests were explored numerically along with the control strategies applied in Saudi Arabia.

Keywords: mathematical model; COVID-19; stability; random diagnoses; lockdown; social distancing; Saudi Arabia

1. Introduction

Coronavirus disease 2019, COVID-19, is a new infectious disease that emerged at the end of 2019. Within three months, became a global epidemic [1]. As of December 26, 2021, the number of confirmed cases around the world had reached 278,714,484 [2]. The epidemic affected various aspects of life, including the economic, health and social aspects.

Several researchers have discussed the disease dynamics and characteristics of COVID-19 patients in different regions of the world. Individuals infected with COVID-19 may or may not have symptoms that range from mild to severe. Individuals who experience a fever, dry cough, fatigue and headaches as mild symptoms or acute respiratory distress syndrome as a severe symptom [3] are called symptomatic

individuals. Individuals who do not show any signs and their infection is confirmed through real-time reverse transcriptase-polymerase chain reaction (RT-PCR), i.e., a type of diagnostic test for COVID-19, are called asymptomatic individuals [4]. These patients can also transmit the disease to other individuals [5, 6].

The presence of asymptomatic patients has led researchers to focus on studying this class of patients. Some research has described the clinical characteristics of asymptomatic and symptomatic patients of COVID-19 [7, 8]. Kim et al. [7] determined the spread of asymptomatic cases in South Korea. Of 213 infected individuals with COVID-19, 41 (19.2%) were asymptomatic. They concluded that as much as one-fifth of infected individuals with COVID-19 are asymptomatic. Therefore, strict social distancing must be applied to prevent the transmission of the disease through these individuals. AlJishi et al. [8] described the spread of COVID-19 at the epicenter of its spread in Saudi Arabia, in the eastern region of the kingdom. They concluded that most COVID-19 cases were asymptomatic and returned from travel. In addition, Alsofayan et al. [9] emphasized the need to give attention to asymptomatic individuals and health care workers because they contribute to the spread of the disease.

Several studies have proposed a mathematical model that considers asymptomatic and symptomatic infected individuals [10–18]. A mathematical model was proposed in [10] to discover the effect of asymptomatic infected people and estimate the number of beds needed in hospitals and intensive care units in Saudi Arabia. They concluded that asymptomatic people are more effective in increasing the number of infections than symptomatic people. However, the increase in COVID-19 testing and social distancing reduces the infection by asymptomatic individuals. Sun and Weng [15] established a mathematical model to discuss the effect of asymptomatic and imported patients in the Jiangsu and Anhui provinces in China. Their analysis found that asymptomatic patients are more dangerous than imported patients. Moreover, asymptomatic patients can rapidly cause an outbreak of the disease without strict preventive measures.

Serhani and Labbardi [16] analyzed two mathematical models to study the spread of COVID-19 in Morocco without and with containment of the pandemic. They found that the free equilibrium point is asymptotically stable when the containment coefficient exceeds the basic reproduction number $\mathcal{R}_0$. Furthermore, increasing the containment rate decreases the number of asymptomatic and symptomatic individuals. Huo et al. [17] studied the spread of COVID-19 and the effect of non-pharmaceutical interventions in Wuhan. They estimated that 20% of patients remain asymptomatic during infection, and that their ability to transmit is around 70% of the symptomatic patients' ability.

Moreover, in [13, 14], the authors analyzed mathematical models for COVID-19 in Saudi Arabia. The models assumed the transmission of infection is due to the environment and occurs through contact with exposed, asymptomatic and symptomatic individuals. Alzahrani et al. [13] dealt with a fractional model. Alqarni et al. [14] used a classical epidemic model and concluded that the cases in Saudi Arabia would decrease if contact with exposed individuals and the environment decreases.

With the increasing number of infections and the contribution of asymptomatic individuals to the transmission of the disease, there have been efforts in various countries to constrain the epidemic. Several precautions have been imposed to keep susceptible individuals away from infected individuals. Studies have demonstrated the effectiveness of preventive measures, such as lockdowns [19–21], social distancing [22–24], quarantining [12, 16] and isolation [25, 26]. Nevertheless, we need measures to detect asymptomatic patients, particularly at the beginning of the disease and before treatment is available, to limit its spread and reduce the number of deaths, an example of such a measure is diagnosis

testing [27].

Al-Salti et al. [18] developed a mathematical model to analyze the optimal control strategies, especially diagnosis and quarantining, for the spread of COVID-19 in the Sultanate of Oman. It was concluded that diagnosis and quarantining are the most important strategies for controlling the disease. Similarly, in [11], Ahmed et al. confirmed the effectiveness of the diagnosis in reducing the infected cases. In addition, Khan et al. [28] studied the effectiveness of Saudi Arabia's experience in producing the diagnosis of COVID-19. From April 14 to mid-July of 2020, the Saudi's diagnostic program for COVID-19 was conducted in three stages [28, 29]. The first stage was performing random diagnostic tests on people in crowded places such as workers' housing, which included 807 locations from April 16 to May 5, 2020 [30]. The second stage was conducting diagnostic tests in specific health centers through an application (Mawid) from May 3 to May 19, 2020. The third stage was conducting rapid tests at medical centers through drive-in vehicles, which started on May 29, 2020 [31, 32]. Also, the government of Saudi Arabia has continued to expand the diagnostic procedures for COVID-19 [33–36].

This paper describe the study of the impact of detecting asymptomatic COVID-19 patients through random diagnostic testing in Saudi Arabia. Random diagnosis means diagnosing COVID-19 for suspected individuals at random, whether they show symptoms or not. In other words, officials in the Ministry of Health go to homes and diagnose individuals in places where there are factors that contribute to the spread of the disease, such as overpopulation.

We extend our model in [37] to include the asymptomatic COVID-19 patients and analyze the impact of random diagnostic tests. Therefore, this model contains three control measures that have been implemented in Saudi Arabia: lockdown, social distancing and random diagnostic testing. The analysis of this model attempts to determine if it is possible to rely on random diagnosis while reducing or eliminating lockdown and social distancing. This paper is organized as follows. In Section 2, we formulate the model and prove that it is well posed. In Section 3, we demonstrate the qualitative analysis, including the equilibrium points, basic and control reproduction numbers, and the local and global stability of the equilibrium points. Section 4 presents the numerical analysis, which includes the fitting of the model to COVID-19 cases in Saudi Arabia and the estimation of the model parameters. Furthermore, we describe numerical experiments that were conducted to confirm the qualitative analysis results and investigate the sensitivity analysis for the control reproduction number. Finally, we analyze different scenarios for control strategies, random diagnostic testing, lockdown and social distancing.

2. Mathematical model

The model was formulated to examine the effect of the random diagnostic tests for asymptomatic patients on the spread of COVID-19 in Saudi Arabia. The Saudi population, N, comprises five compartments: susceptible individuals, S, exposed individuals, E, asymptomatic infected individuals (with no symptoms), I_a, symptomatic infected individuals (with symptoms), I_s, and recovered individuals, R. Individuals move from the susceptible compartment to the exposed compartment after interacting with infected individuals, symptomatic or asymptomatic, at the transmission rates β_1 and β_2, respectively. The control measures, i.e., the lockdown ($\rho(t) \in (0, 1]$) and the social distancing ($SD(t) \in [0, 1)$), impact the transmission rates β_1 and β_2. However, the random diagnostic testing for asymptomatic individuals affects only β_2. The function $\varepsilon(t) \in [0, 1]$ represents the effectiveness of the random diagnostic

testing for I_a. If $\varepsilon = 1$, then the random diagnostic test was administered to all asymptomatic individuals in the community. Conversely, no random diagnostic test is performed for I_a when $\varepsilon = 0$. After completing the incubation period, $1/\gamma$, individuals in the exposed compartment move to the asymptomatic compartment with the probability θ, where $\theta \in (0, 1)$; and the rest of the individuals $(1 - \theta)$ move to the symptomatic compartment. We assume that individuals in the exposed compartment may or may not show symptoms by the end of the incubation period. Also, individuals in the asymptomatic compartment can transmit the disease more than individuals in the symptomatic compartment, that is, $\beta_2 > \beta_1$. Moreover, individuals die due to COVID-19 only from the symptomatic compartment at a rate d. Infected individuals, asymptomatic and symptomatic, recover and gain immunity to COVID-19 at a rate δ. The natural death rate for each compartment is μ, and η is the natural birth rate.

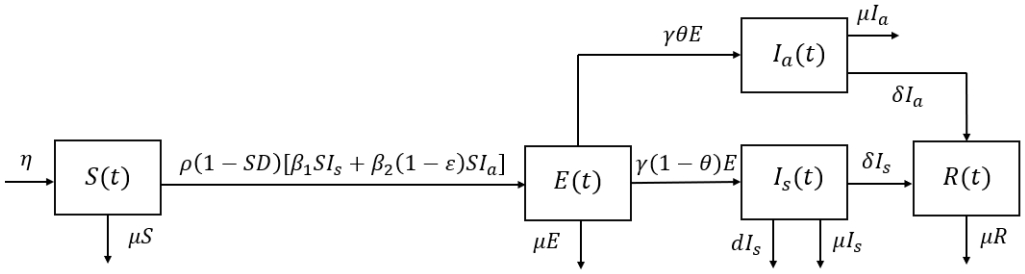

Figure 1. Flowchart of the model.

Figure 1 displays the model's dynamics. We express the model mathematically with the following nonlinear system of ordinary differential equations:

$$\begin{aligned}
\frac{dS}{dt} &= \eta - \rho(1 - SD)[\beta_1 SI_s + \beta_2(1 - \varepsilon)SI_a] - \mu S,\\
\frac{dE}{dt} &= \rho(1 - SD)[\beta_1 SI_s + \beta_2(1 - \varepsilon)SI_a] - (\gamma + \mu)E,\\
\frac{dI_a}{dt} &= \gamma\theta E - (\delta + \mu)I_a,\\
\frac{dI_s}{dt} &= \gamma(1 - \theta)E - (\delta + d + \mu)I_s,\\
\frac{dR}{dt} &= \delta I_a + \delta I_s - \mu R,
\end{aligned} \tag{2.1}$$

where all parameters belong to the interval $(0, 1]$ and $N = S(t) + E(t) + I_a(t) + I_s(t) + R(t)$.

We start the analysis by proving that the state variables of Model (2.1) are epidemiologically meaningful, that is, non-negative and bounded.

Theorem 1

If $(S, E, I_a, I_s, R) \in \mathbb{R}^5_{\geq 0}$, *then the set*

$$\Omega = \left\{(S, E, I_a, I_s, R) \in \mathbb{R}^5_{\geq 0} : 0 \leq N \leq \frac{\eta}{\mu}\right\}$$

is positively invariant for Model (2.1).

Proof.
Let $(S(0), E(0), I_a(0), I_s(0), R(0)) \in \Omega$. We have

$$\begin{aligned}
\frac{dS}{dt}\Big|_{S=0} &= \eta > 0,\\
\frac{dE}{dt}\Big|_{E=0} &= \rho(1 - SD)[\beta_1 S I_s + \beta_2(1-\varepsilon)S I_a] \geq 0, \text{ for all } S,\ I_a,\ I_s \geq 0,\\
\frac{dI_a}{dt}\Big|_{I_a=0} &= \gamma\theta E \geq 0, \text{ for all } E \geq 0,\\
\frac{dI_s}{dt}\Big|_{I_s=0} &= \gamma(1-\theta)E \geq 0, \text{ for all } E \geq 0,\\
\frac{dR}{dt}\Big|_{R=0} &= \delta I_a + \delta I_s \geq 0, \text{ for all } I_a,\ I_s \geq 0.
\end{aligned}$$

Thus, all non-negative solutions remain non-negative for $t \geq 0$. By adding all of the equations of Model (2.1), we get

$$\frac{dN}{dt} = \eta - dI_s - \mu N \leq \eta - \mu N.$$

Multiplying the above inequality by the integrating factor $(e^{\mu r})$, we have

$$\frac{d}{dr}\Big[e^{\mu r}N(r)\Big] \leq \eta e^{\mu r}.$$

By integrating both sides over the interval $[0, t]$, we obtain

$$N(t) \leq \frac{\eta}{\mu} + \Big[N(0) - \frac{\eta}{\mu}\Big]e^{-\mu t}.$$

Hence,

$$\lim_{t\to\infty} Sup\Big[N(t)\Big] \leq \frac{\eta}{\mu}.$$

Therefore, for $t \geq 0$, the solutions of Model (2.1) are non-negative and bounded. Thus, Ω is positively invariant. □

3. Qualitative analysis

We qualitatively investigate Model (2.1). First, we determine the equilibrium points and the expression of the control reproduction number. Second, we examine the local and global stability of the equilibrium points.

3.1. Equilibrium points and control reproduction number

The equilibrium points of the model are determined by setting the rates for Model (2.1) to zero:

$$\begin{aligned}
\eta - \rho(1 - SD)[\beta_1 S I_s + \beta_2(1-\varepsilon)S I_a] - \mu S &= 0,\\
\rho(1 - SD)[\beta_1 S I_s + \beta_2(1-\varepsilon)S I_a] - (\gamma + \mu)E &= 0,\\
\gamma\theta E - (\delta + \mu)I_a &= 0,
\end{aligned} \tag{3.1}$$

$$\gamma(1-\theta)E-(\delta+d+\mu)I_s=0,$$
$$\delta I_a+\delta I_s-\mu R=0.$$

System (3.1) produces two steady-state solutions: the COVID-19 free equilibrium point, $P_0 = (\eta/\mu, 0, 0, 0, 0)$, which always exists, and the COVID-19 endemic equilibrium point, $P_1 = (S_1, E_1, I_{a_1}, I_{s_1}, R_1)$, where

$$S_1=\frac{\eta}{\mu\mathcal{R}_c},\qquad I_{a_1}=\frac{\eta\gamma\theta}{(\gamma+\mu)(\delta+\mu)}\left(1-\frac{1}{\mathcal{R}_c}\right),$$
$$E_1=\frac{\eta}{(\gamma+\mu)}\left(1-\frac{1}{\mathcal{R}_c}\right),\qquad I_{s_1}=\frac{\eta\gamma(1-\theta)}{(\gamma+\mu)(\delta+d+\mu)}\left(1-\frac{1}{\mathcal{R}_c}\right),$$
$$R_1=\frac{\eta\gamma(\delta\theta d+\delta^2+\delta\mu)}{\mu(\gamma+\mu)(\delta+\mu)(\delta+d+\mu)}\left(1-\frac{1}{\mathcal{R}_c}\right).$$

Here,

$$\mathcal{R}_c=\frac{\rho(1-SD)\beta_1(1-\theta)\gamma\eta}{\mu(\gamma+\mu)(\delta+d+\mu)}+\frac{\rho(1-SD)\beta_2\theta(1-\varepsilon)\gamma\eta}{\mu(\gamma+\mu)(\delta+\mu)}.$$

The endemic equilibrium P_1 exists only if $\mathcal{R}_c > 1$.

Control reproduction number. We use the next-generation matrix method [38] to find the control reproduction number. Let the infected compartments $O = (E, I_a, I_s)^T$; then, the exposed class, asymptomatic class and symptomatic class equations of Model (2.1) can be rewritten as $\dot{O} = \mathscr{F}(O) - \mathscr{V}(O)$, where

$$\mathscr{F}=\begin{bmatrix}\rho(1-SD)[\beta_1 SI_s+\beta_2(1-\varepsilon)SI_a]\\0\\0\end{bmatrix}$$

and

$$\mathscr{V}=\begin{bmatrix}(\gamma+\mu)E\\-\gamma\theta E+(\delta+\mu)I_a\\-\gamma(1-\theta)E+(\delta+d+\mu)I_s\end{bmatrix}.$$

Evaluating the Jacobian matrix of $\mathscr{F}$ and $\mathscr{V}$ at the COVID-19 free equilibrium point P_0, we get, respectively,

$$F=\begin{bmatrix}0&\dfrac{\rho(1-SD)\beta_2(1-\varepsilon)\eta}{\mu}&\dfrac{\rho(1-SD)\beta_1\eta}{\mu}\\0&0&0\\0&0&0\end{bmatrix}$$

and

$$V=\begin{bmatrix}\gamma+\mu&0&0\\-\gamma\theta&\delta+\mu&0\\-\gamma(1-\theta)&0&\delta+d+\mu\end{bmatrix}.$$

The next-generation matrix is

$$FV^{-1}=\begin{bmatrix}K_1&\dfrac{\rho(1-SD)\beta_2(1-\varepsilon)\eta}{\mu(\delta+\mu)}&\dfrac{\rho(1-SD)\beta_1\eta}{\mu(\delta+d+\mu)}\\0&0&0\\0&0&0\end{bmatrix},$$

where

$$K_1 = \frac{\rho(1 - SD)\beta_1(1 - \theta)\gamma\eta}{\mu(\gamma + \mu)(\delta + d + \mu)} + \frac{\rho(1 - SD)\beta_2\theta(1 - \varepsilon)\gamma\eta}{\mu(\gamma + \mu)(\delta + \mu)}.$$

Hence, the control reproduction number is the spectral radius of the matrix FV^{-1}, that is,

$$\mathcal{R}_c = \frac{\rho(1 - SD)\beta_1(1 - \theta)\gamma\eta}{\mu(\gamma + \mu)(\delta + d + \mu)} + \frac{\rho(1 - SD)\beta_2\theta(1 - \varepsilon)\gamma\eta}{\mu(\gamma + \mu)(\delta + \mu)}. \tag{3.2}$$

Also, we can rewrite Expression (3.2) as follows: $\mathcal{R}_c = \rho(1 - SD)\left(\mathcal{R}_s + (1 - \varepsilon)\mathcal{R}_a\right)$, where $\mathcal{R}_s$ gives the secondary cases of COVID-19 by one symptomatic individuals, and $\mathcal{R}_a$ gives the secondary cases of COVID-19 by one asymptomatic individuals.

The terms in $\mathcal{R}_c$ are explained further as follows. First, for $\mathcal{R}_s$, the term that expresses the incidence of new infections by symptomatic individuals is $\beta_1 S I_s$. Thus, the number of secondary cases by one symptomatic individual ($I_s = 1$) in a population containing only susceptible individuals is $\beta_1 S_0$, where $S_0 = \eta/\mu$. Moreover, $1/(\delta + d + \mu)$ represents the average time spent by one symptomatic individual in the symptomatic compartment. Also, $\gamma(1 - \theta)/(\gamma + \mu)$ is the proportion of newly symptomatic individuals that survived the incubation period. Second, for $\mathcal{R}_a$, the term that represents the incidence of new infections by asymptomatic individuals is $\beta_2 S I_a$. Therefore, the number of secondary cases by one asymptomatic individual ($I_a = 1$) in a population containing only susceptible individuals is $\beta_2 S_0$, where $S_0 = \eta/\mu$. Further, $1/(\delta+\mu)$ expresses the average time spent by one asymptomatic individual in the asymptomatic compartment. Again, $\gamma\theta/(\gamma+\mu)$ is the proportion of newly asymptomatic individuals that survived the incubation period.

3.2. Local stability analysis

We employ the linearization method [39] to examine the local stability of the equilibrium points of Model (2.1).

Theorem 2

The COVID-19 free equilibrium point P_0 is locally asymptotically stable if $\mathcal{R}_c < 1$.

Proof.

The Jacobian matrix of Model (2.1) evaluated at P_0 yields

$$J(P_0) = \begin{bmatrix} -\mu & 0 & -\rho(1 - SD)\beta_2(1 - \varepsilon)S_0 & -\rho(1 - SD)\beta_1 S_0 & 0 \\ 0 & -(\gamma + \mu) & \rho(1 - SD)\beta_2(1 - \varepsilon)S_0 & \rho(1 - SD)\beta_1 S_0 & 0 \\ 0 & \gamma\theta & -(\delta + \mu) & 0 & 0 \\ 0 & \gamma(1 - \theta) & 0 & -(\delta + d + \mu) & 0 \\ 0 & 0 & \delta & \delta & -\mu \end{bmatrix}.$$

By solving the characteristic equation $\mid J(P_0) - \lambda I \mid = 0$, we obtain the eigenvalues $\lambda_{1,2} = -\mu$, and $\lambda_{3,4,5}$ are roots of the following equation:

$$\lambda^3 + a_1\lambda^2 + a_2\lambda + a_3 = 0,$$

where

$$a_1 = \gamma + d + 2\delta + 3\mu,$$

$$
\begin{aligned}
a_2 &= (\delta+\mu)(\delta+d+\mu) + (\gamma+\mu)(\delta+\mu)[1-\rho(1-SD)(1-\varepsilon)\mathcal{R}_a] \\
&\quad + (\gamma+\mu)(\delta+d+\mu)[1-\rho(1-SD)\mathcal{R}_s], \\
a_3 &= (\gamma+\mu)(\delta+\mu)(\delta+d+\mu)(1-\mathcal{R}_c).
\end{aligned}
$$

We use the Routh-Hurwitz criteria [39] to determine the signs of the remaining eigenvalues $\lambda_{3,4,5}$. They are negative if $a_1 > 0, a_3 > 0$ and $a_1a_2 - a_3 > 0$. Clearly, $a_1 > 0$. Also, $a_3 > 0$ if $\mathcal{R}_c < 1$. Moreover,

$$
\begin{aligned}
a_1a_2 - a_3 &= 2(\gamma+\mu)(\delta+\mu)(\delta+d+\mu) + (\delta+\mu)^2(\delta+d+\mu) + (\delta+\mu)(\delta+d+\mu)^2 \\
&\quad + \left((\gamma+\mu)^2(\delta+d+\mu) + (\gamma+\mu)(\delta+d+\mu)^2\right)[1-\rho(1-SD)\mathcal{R}_s] \\
&\quad + \left((\gamma+\mu)^2(\delta+\mu) + (\gamma+\mu)(\delta+\mu)^2\right)[1-\rho(1-SD)(1-\varepsilon)\mathcal{R}_a].
\end{aligned}
$$

If $\mathcal{R}_c = \rho(1-SD)[\mathcal{R}_s + (1-\varepsilon)\mathcal{R}_a] < 1$, then $\rho(1-SD)\mathcal{R}_s < 1$ and $\rho(1-SD)(1-\varepsilon)\mathcal{R}_a < 1$. Thus, $a_1a_2 - a_3 > 0$. Hence, P_0 is locally asymptotically stable if $\mathcal{R}_c < 1$. □

Theorem 3

The COVID-19 endemic equilibrium point P_1 is locally asymptotically stable if $\mathcal{R}_c > 1$.

Proof.

The Jacobian matrix of Model (2.1) evaluated at P_1 yields

$$
J(P_1) = \begin{bmatrix}
J_{11} & 0 & -\rho(1-SD)\beta_2(1-\varepsilon)S_1 & -\rho(1-SD)\beta_1 S_1 & 0 \\
J_{21} & -(\gamma+\mu) & \rho(1-SD)\beta_2(1-\varepsilon)S_1 & \rho(1-SD)\beta_1 S_1 & 0 \\
0 & \gamma\theta & -(\delta+\mu) & 0 & 0 \\
0 & \gamma(1-\theta) & 0 & -(\delta+d+\mu) & 0 \\
0 & 0 & \delta & \delta & -\mu
\end{bmatrix},
$$

where

$$
\begin{aligned}
J_{11} &= -\rho(1-SD)[\beta_1 I_{s_1} + \beta_2(1-\varepsilon)I_{a_1}] - \mu, \\
J_{21} &= \rho(1-SD)[\beta_1 I_{s_1} + \beta_2(1-\varepsilon)I_{a_1}].
\end{aligned}
$$

The characteristic equation, $| J(P_1) - \lambda I | = 0$, has the eigenvalues $\lambda_1 = -\mu$, and $\lambda_{2,3,4,5}$ are the roots of the following equation:

$$
\lambda^4 + a_1\lambda^3 + a_2\lambda^2 + a_3\lambda + a_4 = 0, \tag{3.3}
$$

where

$$
\begin{aligned}
a_1 &= \mu\mathcal{R}_c + \gamma + d + 2\delta + 3\mu, \\
a_2 &= \mu(\delta+d+\mu)\mathcal{R}_c + \mu(\gamma+\delta+2\mu)\mathcal{R}_c + (\delta+\mu)(\delta+d+\mu) \\
&\quad + (\gamma+\mu)(\delta+\mu)\Big[1 - \frac{\rho(1-SD)(1-\varepsilon)\mathcal{R}_a}{\mathcal{R}_c}\Big] \\
&\quad + (\gamma+\mu)(\delta+d+\mu)\Big[1 - \frac{\rho(1-SD)\mathcal{R}_s}{\mathcal{R}_c}\Big], \\
a_3 &= \mu(\gamma+\mu)(\delta+\mu)(\delta+d+\mu)\mathcal{R}_c + \mu(\delta+\mu)(\delta+d+\mu)\mathcal{R}_c \\
&\quad + \eta\gamma\rho(1-SD)[\beta_1(1-\theta) + \beta_2\theta(1-\varepsilon)]\left(1 - \frac{1}{\mathcal{R}_c}\right),
\end{aligned}
$$

$$a_4 = \mu(\gamma+\mu)(\delta+\mu)(\delta+d+\mu)\mathcal{R}_c.$$

Clearly, $a_1 > 0$ and $a_4 > 0$. Also, since $\mathcal{R}_c = \rho(1-SD)(\mathcal{R}_s+(1-\varepsilon)\mathcal{R}_a) > 1$, then $a_2 > 0$ and $a_3 > 0$. By the Descartes' rule [40], the characteristic equation given by Eq (3.3) has no positive roots since there is no change in the signs of the coefficients. When substituting for (λ) by $(-\lambda)$ in Eq (3.3), the signs of the coefficients change as follows:

$$\lambda^4 - a_1\lambda^3 + a_2\lambda^2 - a_3\lambda + a_4 = 0.$$

The number of sign changes is four; therefore, the characteristic Eq (3.3) has four negative eigenvalues. Hence, P_1 is locally asymptotically stable if $\mathcal{R}_c > 1$. □

3.3. Global stability analysis

We utilize the Lyapunov and Krasovkii–LaSalle stability theorems [41–43] to examine the global stability of the equilibrium points of Model (2.1). Also, we use the function $W(u) = u - 1 - \ln u$, which is a positive function, in the following proofs.

Theorem 4
The COVID-19 free equilibrium point P_0 is globally asymptotically stable if $\mathcal{R}_c < 1$.

Proof.
Define the Lyapunov function $L_0(S, E, I_a, I_s, R)$ as follows:

$$\begin{aligned}
L_0 = {} & S_0 W(S/S_0) + E + \frac{(\gamma+\mu)}{\gamma}\left[\frac{\rho(1-SD)(1-\varepsilon)}{\theta}\mathcal{R}_a + \frac{(\delta+d+\mu)}{(\theta d+\delta+\mu)}(1-\mathcal{R}_c)\right]I_a \\
& + \frac{(\gamma+\mu)}{\gamma}\left[\frac{\rho(1-SD)}{(1-\theta)}\mathcal{R}_s + \frac{(\delta+\mu)}{(\theta d+\delta+\mu)}(1-\mathcal{R}_c)\right]I_s \\
& + \frac{(\gamma+\mu)(\delta+\mu)(\delta+d+\mu)}{\gamma\delta(\theta d+\delta+\mu)}(1-\mathcal{R}_c)R.
\end{aligned}$$

If $\mathcal{R}_c < 1$, then L_0 is positive-definite since $L_0(S, E, I_a, I_s, R) > 0$ for all $(S, E, I_a, I_s, R) \in \Omega$ and $L_0(P_0) = 0$. Computing the time derivative of L_0 along the solutions of Model (2.1), we get

$$\begin{aligned}
\frac{dL_0}{dt} = {} & \left(1-\frac{S_0}{S}\right)[\eta - \rho(1-SD)[\beta_1 S I_s + \beta_2(1-\varepsilon)S I_a] - \mu S] \\
& + [\rho(1-SD)[\beta_1 S I_s + \beta_2(1-\varepsilon)S I_a] - (\gamma+\mu)E] \\
& + \frac{(\gamma+\mu)}{\gamma}\left[\frac{\rho(1-SD)(1-\varepsilon)}{\theta}\mathcal{R}_a + \frac{(\delta+d+\mu)}{(\theta d+\delta+\mu)}(1-\mathcal{R}_c)\right][\gamma\theta E - (\delta+\mu)I_a] \\
& + \frac{(\gamma+\mu)}{\gamma}\left[\frac{\rho(1-SD)}{(1-\theta)}\mathcal{R}_s + \frac{(\delta+\mu)}{(\theta d+\delta+\mu)}(1-\mathcal{R}_c)\right][\gamma(1-\theta)E - (\delta+d+\mu)I_s] \\
& + \frac{(\gamma+\mu)(\delta+\mu)(\delta+d+\mu)}{\gamma\delta(\theta d+\delta+\mu)}(1-\mathcal{R}_c)[\delta I_a + \delta I_s - \mu R].
\end{aligned}$$

Since $S_0 = \eta/\mu$, then $\eta = \mu S_0$. Collecting terms, we get

$$\begin{aligned}\frac{dL_0}{dt} &= \left(1 - \frac{S_0}{S}\right)(\mu S_0 - \mu S) - \frac{\mu(\gamma+\mu)(\delta+\mu)(\delta+d+\mu)}{\gamma\delta(\theta d+\delta+\mu)}(1-\mathcal{R}_c)R \\ &- \left[(\gamma+\mu) - \theta(\gamma+\mu)\left(\frac{\rho(1-SD)(1-\varepsilon)}{\theta}\mathcal{R}_a + \frac{(\delta+d+\mu)}{(\theta d+\delta+\mu)}(1-\mathcal{R}_c)\right)\right. \\ &\left. - (1-\theta)(\gamma+\mu)\left(\frac{\rho(1-SD)}{(1-\theta)}\mathcal{R}_s + \frac{(\delta+\mu)}{(\theta d+\delta+\mu)}(1-\mathcal{R}_c)\right)\right]E \\ &- \left[\frac{(\gamma+\mu)(\delta+\mu)}{\gamma}\left(\frac{\rho(1-SD)(1-\varepsilon)}{\theta}\mathcal{R}_a + \frac{(\delta+d+\mu)}{(\theta d+\delta+\mu)}(1-\mathcal{R}_c)\right)\right. \\ &\left. - \rho(1-SD)\beta_2(1-\varepsilon)S_0 - \frac{(\gamma+\mu)(\delta+\mu)(\delta+d+\mu)}{\gamma(\theta d+\delta+\mu)}(1-\mathcal{R}_c)\right]I_a \\ &- \left[\frac{(\gamma+\mu)(\delta+d+\mu)}{\gamma}\left(\frac{\rho(1-SD)}{(1-\theta)}\mathcal{R}_s + \frac{(\delta+\mu)}{(\theta d+\delta+\mu)}(1-\mathcal{R}_c)\right)\right. \\ &\left. - \rho(1-SD)\beta_1 S_0 - \frac{(\gamma+\mu)(\delta+\mu)(\delta+d+\mu)}{\gamma(\theta d+\delta+\mu)}(1-\mathcal{R}_c)\right]I_s.\end{aligned}$$

After simplifications by using expressions of $\mathcal{R}_a$ and $\mathcal{R}_s$, we obtain

$$\frac{dL_0}{dt} = -\frac{\mu(S-S_0)^2}{S} - \frac{\mu(\gamma+\mu)(\delta+\mu)(\delta+d+\mu)}{\gamma\delta(\theta d+\delta+\mu)}(1-\mathcal{R}_c)R.$$

If $\mathcal{R}_c < 1$, then $dL_0/dt \leq 0$ for all $S, R > 0$. Also, $dL_0/dt = 0$ when $S(t) = S_0$, and $R(t) = 0$. Applying the Krasovkii-Lasalle theorem, we suppose that

$$\mathscr{I}_0 = \left\{(S(t), E(t), I_a(t), I_s(t), R(t)) : \frac{dL_0}{dt} = 0\right\},$$

and M_0 is the largest invariant subset of $\mathscr{I}_0$, where all elements in it satisfy $S(t) = S_0$ and $R(t) = 0$. Then, from the fifth equation of Model (2.1), we get

$$\frac{dR}{dt} = 0 = \delta(I_a + I_s) \quad \Longrightarrow \quad I_a(t) = 0 \text{ and } I_s(t) = 0.$$

Substituting this into the third equation of Model (2.1), we have

$$\frac{dI_a}{dt} = 0 = \gamma\theta E \quad \Longrightarrow \quad E(t) = 0.$$

Hence, $M_0 = \{P_0\}$; thus, the equilibrium P_0 is globally asymptotically stable if $\mathcal{R}_c < 1$. □

Theorem 5

The COVID-19 endemic equilibrium point P_1 is globally asymptotically stable if $\mathcal{R}_c > 1$.

Proof.

Define the Lyapunov function $L_1(S, E, I_a, I_s, R)$ as follows:

$$\begin{aligned}L_1 &= S_1 W(S/S_1) + E_1 W(E/E_1) + \frac{\eta\rho(1-SD)\beta_2(1-\varepsilon)}{\mu(\delta+\mu)\mathcal{R}_c} I_{a_1} W(I/I_{a_1}) \\ &+ \frac{\eta\rho(1-SD)\beta_1}{\mu(\delta+d+\mu)\mathcal{R}_c} I_{s_1} W(I/I_{s_1}).\end{aligned}$$

Clearly, $L_1(S, E, I_a, I_s, R)$ is a positive semi-definite function since $L_1 \geq 0$ for all $(S, E, I_a, I_s, R) \in \Omega$ and $L_1(S_1, E_1, I_{a_1}, I_{s_1}, R_1) = 0$. The time derivative of L_1 along the solutions of Model (2.1) is given by

$$\begin{aligned}\frac{dL_1}{dt} &= \left(1 - \frac{S_1}{S}\right)\Big[\eta - \rho(1 - SD)[\beta_1 S I_s + \beta_2(1-\varepsilon)S I_a] - \mu S\Big] \\ &\quad + \left(1 - \frac{E_1}{E}\right)\Big[\rho(1 - SD)[\beta_1 S I_s + \beta_2(1-\varepsilon)S I_a] - (\gamma + \mu)E\Big] \\ &\quad + \left(1 - \frac{I_{a_1}}{I_a}\right)\frac{\eta\rho(1 - SD)\beta_2(1-\varepsilon)}{\mu(\delta + \mu)\mathcal{R}_c}\Big[\gamma\theta E - (\delta + \mu)I_a\Big] \\ &\quad + \left(1 - \frac{I_{s_1}}{I_s}\right)\frac{\eta\rho(1 - SD)\beta_1}{\mu(\delta + d + \mu)\mathcal{R}_c}\Big[\gamma(1-\theta)E - (\delta + d + \mu)I_s\Big].\end{aligned}$$

From the equilibrium described by Eq (3.1) for P_1, we have

$$\begin{aligned}\eta &= \rho(1 - SD)[\beta_1 S_1 I_{s_1} + \beta_2(1-\varepsilon)S_1 I_{a_1}] + \mu S_1, \\ (\gamma + \mu)E_1 &= \rho(1 - SD)[\beta_1 S_1 I_{s_1} + \beta_2(1-\varepsilon)S_1 I_{a_1}].\end{aligned}$$

Then,

$$\begin{aligned}\frac{dL_1}{dt} &= -\frac{\mu(S - S_1)^2}{S} + 3\rho(1 - SD)[\beta_1 S_1 I_{s_1} + \beta_2(1-\varepsilon)S_1 I_{a_1}] \\ &\quad + \Big[\frac{\gamma(1-\theta)\rho(1 - SD)\beta_1 S_1}{(\delta + d + \mu)} + \frac{\gamma\theta\rho(1 - SD)\beta_2(1-\varepsilon)S_1}{(\delta + \mu)} - (\gamma + \mu)\Big]E \\ &\quad - \rho(1 - SD)\beta_1 S_1 I_{s_1}\frac{S_1}{S} - \rho(1 - SD)\beta_2(1-\varepsilon)S_1 I_{a_1}\frac{S_1}{S} \\ &\quad - \rho(1 - SD)\beta_1 S I_s\frac{S_1 I_{s_1} E_1}{S_1 I_{s_1} E} - \rho(1 - SD)\beta_2(1-\varepsilon)S I_a\frac{S_1 I_{a_1} E_1}{S_1 I_{a_1} E} \\ &\quad - \frac{\gamma\theta\rho(1 - SD)\beta_2(1-\varepsilon)S_1}{(\delta + \mu)}\,\frac{E_1 I_{a_1} E I_{a_1}}{E_1 I_{a_1} I_a} - \frac{\gamma(1-\theta)\rho(1 - SD)\beta_1 S_1}{(\delta + d + \mu)}\,\frac{E_1 I_{s_1} E I_{s_1}}{E_1 I_{s_1} I_s}.\end{aligned} \tag{3.4}$$

Now, we substitute for $S_1 = \eta/\mu\mathcal{R}_c$ in the coefficient of E in Eq (3.4) and use the formula of $\mathcal{R}_c$. Moreover, we substitute the values of E_1, $1/I_{a_1}$ and $1/I_{s_1}$ in the following terms:

$$\begin{aligned}\left(\frac{\gamma\theta E_1}{(\delta + \mu)I_{a_1}}\right)\rho(1 - SD)\beta_2(1-\varepsilon)S_1 I_{a_1}\frac{E I_{a_1}}{E_1 I_a} &= \rho(1 - SD)\beta_2(1-\varepsilon)S_1 I_{a_1}\frac{E I_{a_1}}{E_1 I_a}, \\ \left(\frac{\gamma(1-\theta)E_1}{(\delta + d + \mu)I_{s_1}}\right)\rho(1 - SD)\beta_1 S_1 I_{s_1}\frac{E I_{s_1}}{E_1 I_s} &= \rho(1 - SD)\beta_1 S_1 I_{s_1}\frac{E I_{s_1}}{E_1 I_s}.\end{aligned}$$

After simplifying Eq (3.4), we obtain

$$\begin{aligned}\frac{dL_1}{dt} &= -\frac{\mu(S - S_1)^2}{S} + \rho(1 - SD)\beta_2(1-\varepsilon)S_1 I_{a_1}\left(3 - \frac{S_1}{S} - \frac{S I_a E_1}{S_1 I_{a_1} E} - \frac{E I_{a_1}}{E_1 I_a}\right) \\ &\quad + \rho(1 - SD)\beta_1 S_1 I_{s_1}\left(3 - \frac{S_1}{S} - \frac{S I_s E_1}{S_1 I_{s_1} E} - \frac{E I_{s_1}}{E_1 I_s}\right).\end{aligned}$$

Since the arithmetic mean is greater than or equal to the geometric mean, we have

$$3 - \frac{S_1}{S} - \frac{SI_aE_1}{S_1I_{a_1}E} - \frac{EI_{a_1}}{E_1I_a} \leq 0,$$
$$3 - \frac{S_1}{S} - \frac{SI_sE_1}{S_1I_{s_1}E} - \frac{EI_{s_1}}{E_1I_s} \leq 0.$$

Hence, $dL_1/dt \leq 0$ for all $S, E, I_a, I_s > 0$ and $dL_1/dt = 0$ when $S(t) = S_1,\ E(t) = E_1,\ I_a(t) = I_{a_1}$ and $I_s(t) = I_{s_1}$. Applying the Krasovkii-Lasalle theorem, we consider the set

$$\mathscr{I}_1 = \left\{(S(t), E(t), I_a(t), I_s(t), R(t)) : \frac{dL_1}{dt} = 0\right\},$$

and M_1 is the largest invariant subset of $\mathscr{I}_1$, where all elements satisfy $S(t) = S_1,\ E(t) = E_1,\ I_a(t) = I_{a_1}$ and $I_s(t) = I_{s_1}$; it remains to be proven that $R(t) = R_1$. Assume that $(S(t), E(t), I_a(t), I_s(t), R(t))$ is a solution to Model (2.1) belonging to the set M_1; thus, we have

$$\frac{dR}{dt} = \delta(I_{a_1} + I_{s_1}) - \mu R. \tag{3.5}$$

Solving Eq (3.5) by using the integrating factor method, we obtain

$$R(t) = R_1 + (R(0) - R_1)e^{-\mu t}. \tag{3.6}$$

Note that, $\delta(I_{a_1} + I_{s_1})/\mu = R_1$. From Eq (3.6), as time increases, $R(t)$ approaches R_1, that is, $\lim_{t\to\infty} R(t) \longrightarrow R_1$. The solution $(S(t), E(t), I_a(t), I_s(t), R(t))$ will stay at the set M_1; hence, $M_1 = \{P_1\}$. Therefore, the equilibrium P_1 is globally asymptotically stable if $\mathcal{R}_c > 1$. □

4. Numerical analysis

Here, we fit Model (2.1) to the actual data of COVID-19 cases in Saudi Arabia and estimate the parameters that make it compatible with reality. Also, we perform numerical experiments to demonstrate the agreement with the qualitative results. Furthermore, we discuss the sensitivity analysis for the control reproduction number, $\mathcal{R}_c$. Finally, we examine different scenarios for the control measures in the model, namely, lockdown, social distancing and the detection of asymptomatic individuals through random diagnostic testing.

Table 1. Descriptions and values of the parameters of Model (2.1).

Parameter	Description	Value	Unit	Source
N	Population of Saudi Arabia	34218169	*Individual*	[44]
η	Birth rate	1250	$Individual \times Day^{-1}$	[37]
μ	Natural death rate	3.6529×10^{-5}	Day^{-1}	[37]
β_1	Transmission rate by I_s	0.0554×10^{-7}	$(Individual \times Day)^{-1}$	Estimated
β_2	Transmission rate by I_a	1.0596×10^{-7}	$(Individual \times Day)^{-1}$	Estimated
γ	Incubation rate	1/6	Day^{-1}	[9]
θ	Probability of becoming I_a	0.54	–	Estimated
ε	Effectiveness of random diagnostic testing for I_a	0	–	Estimated
δ	Recovery rate	3.2772×10^{-1}	Day^{-1}	[37]
d	Death rate due to COVID-19	2.3724×10^{-1}	Day^{-1}	[37]

Table 2. Estimated values for ρ and SD in Model (2.1), with corresponding values of $\mathcal{R}_c$ [37].

Phase	Time	ρ	SD	$\mathcal{R}_c$
Phase 1	$t1 = [12, 22]$	0.85	0.15	4.4267
Phase 2	$t2 = [22, 25]$	0.75	0.30	3.2166
	$t3 = [25, 28]$	0.65	0.45	2.1904
	$t4 = [28, 36]$	0.60	0.55	1.6543
Phase 3	$t5 = [36, 56]$	0.55	0.55	1.5164
Phase 4	$t6 = [56, 67]$	0.55	0.60	1.3479
	$t7 = [67, 83]$	0.55	0.69	1.0446
Phase 5	$t8 = [83, 88]$	0.40	0.80	0.4902
Phase 6	$t9 = [88, 92]$	0.65	0.70	1.1947
	$t10 = [92, 112]$	0.75	0.70	1.3785
Phase 7	$t11 = [112, 120]$	0.80	0.76	1.1764
	$t12 = [120, 130]$	0.80	0.80	0.9803
	$t13 = [130, 144]$	0.80	0.82	0.8823
	$t14 = [144, 169]$	0.85	0.83	0.8853
	$t15 = [169, 179]$	0.85	0.82	0.9374
	$t16 = [179, 193]$	0.90	0.82	0.9926
	$t17 = [193, 204]$	0.95	0.85	0.8731
	$t18 = [204, 207]$	0.95	0.88	0.6985

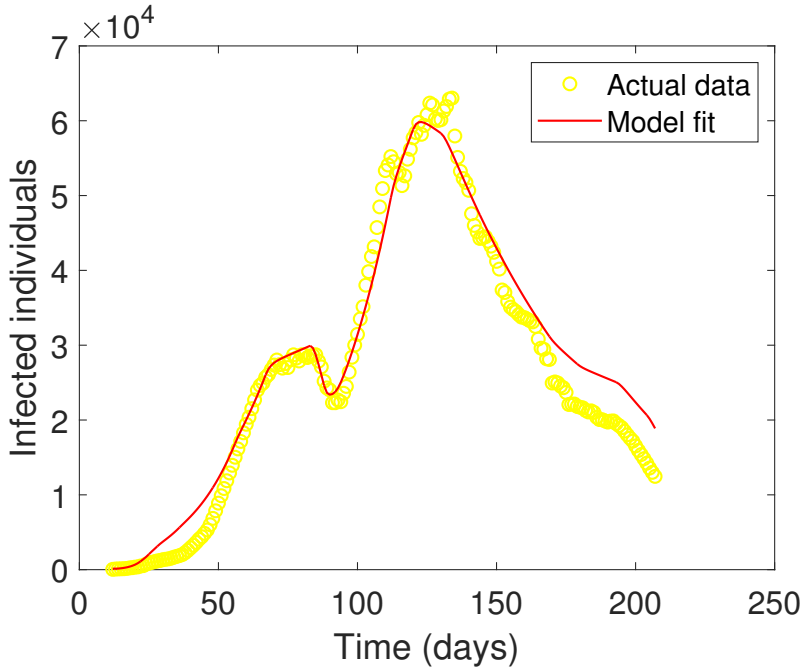

Figure 2. Fitting Model (2.1) for COVID-19 infected cases in Saudi Arabia from March 12, 2020 to September 23, 2020.

4.1. Model fitting and estimation of parameters

We estimate the parameters of Model (2.1) to validate it with the actual data of infected cases in Saudi Arabia. The data of the infected cases were taken from the COVID-19 dashboard of the Saudi Ministry of Health for the period of March 12, 2020 to September 23, 2020 [45].

The health care workers in the Saudi Ministry of Health have applied random diagnostic testing for asymptomatic and symptomatic individuals in dense regions. The random diagnostic tests were done between April 16, 2020 and May 3, 2020, for 42,765 individuals. The number of confirmed cases (positive test result) was 7,776 (18.18%) individuals [28]. We estimate that the effectiveness of the random diagnostic tests for the asymptomatic individuals, ε, to be approximately zero because of the insufficient information about the number of asymptomatic individuals at the time of implementing these tests. Also, the period for these tests is small compared to the time interval of the data considered from the COVID-19 dashboard.

The parameters $\eta,\ \mu, \delta,\ d,\ \rho,\ SD$ and γ have the same values as in [37]. As for the values of the remaining parameters of Model (2.1), we estimate the value of β_2 to be greater than β_1 based on the model's assumption, which is similar to [10, 13].

The parameter values are presented in Table 1. In Table 2, we display the values of lockdown, ρ, social distancing, SD and the corresponding values of $\mathcal{R}_c$. These values were taken from [37], where Saudi Arabia implemented different levels of lockdown and social distancing, which led to dividing the study period into seven phases.

Model (2.1) was solved numerically by using the MATLAB package ode45 with the following initial values: $S(0) = 34813577,\ E(0) = 150,\ I_a(0) = 95,\ I_S(0) = 44$ and $R(0) = 1$. We assumed that each initial value for the exposed class was set to be greater than those for the infected classes, as in [13, 23, 46]. Also, each initial value of the asymptomatic class was set to be greater than those for the symptomatic class based on the results in [8], which demonstrated that most of the COVID-19 cases at the beginning of the spread in Saudi Arabia were asymptomatic and returning from imported. Moreover, Li et al. [6] estimated the undocumented infections (infections with mild, limited or loss of symptoms) to be 86% of the infections in China before imposing travel restrictions on January 23, 2020.

The results of fitting Model (2.1) to the COVID-19 infected cases (symptomatic and asymptomatic) in Saudi Arabia from March 12, 2020 to September 23, 2020 are illustrated in Figure 2, which shows good agreement.

4.2. Numerical experiments

This section demonstrates the agreement between the numerical solution of Model (2.1) and the qualitative analysis offered in Section 3. We conducted numerical simulations of the model for different initial values in the feasible set to show the tendency of the solution curves to equilibrium P_0 if $\mathcal{R}_c < 1$, or equilibrium P_1 if $\mathcal{R}_c > 1$. We start by rescaling the state variables in the model. Let

$$S = \bar{S}N,\ E = \bar{E}N,\ I_a = \bar{I}_aN,\ I_s = \bar{I}_sN,\ R = \bar{R}N. \tag{4.1}$$

Thus, the rescaled Model (2.1) becomes (omitting the bar onward)

$$\begin{aligned}
\frac{dS}{dt} &= \mu - \rho(1 - SD)\frac{\eta}{\mu}\Big[\beta_1 S I_s + \beta_2(1-\varepsilon)S I_a\Big] - \mu S,\\
\frac{dE}{dt} &= \rho(1 - SD)\frac{\eta}{\mu}\Big[\beta_1 S I_s + \beta_2(1-\varepsilon)S I_a\Big] - (\gamma + \mu)E,\\
\frac{dI_a}{dt} &= \gamma\theta E - (\delta + \mu)I_a,\\
\frac{dI_s}{dt} &= \gamma(1-\theta)E - (\delta + d + \mu)I_s,\\
\frac{dR}{dt} &= \delta(I_a + I_s) - \mu R.
\end{aligned} \tag{4.2}$$

Note that we have used the limiting value of N in the model, i.e., $N = \eta/\mu$. We numerically solve Model (4.2) with parameters chosen to satisfy the stability conditions from the qualitative analysis, and with the following different initial conditions belonging to the set Ω:
IC1: $S(0) = 0.8,\ E(0) = 0.1,\ I_a(0) = 0.05,\ I_s(0) = 0.02,\ R(0) = 0.01$,
IC2: $S(0) = 0.6,\ E(0) = 0.2,\ I_a(0) = 0.08,\ I_s(0) = 0.07,\ R(0) = 0.05$,
IC3: $S(0) = 0.4,\ E(0) = 0.3,\ I_a(0) = 0.12,\ I_s(0) = 0.10,\ R(0) = 0.07$.

Experiment 1: Assume the parameters of Model (4.2) have the following values: $\mu = 0.04$, $\eta = 1250$, $\gamma = 0.167$, $\beta_1 = 0.0554 \times 10^{-4}$, $\beta_2 = 1.0596 \times 10^{-4}$, $\varepsilon = 0.50$, $\theta = 0.54$, $\delta = 3.2772 \times 10^{-1}$, $d = 2.3724 \times 10^{-1}$, $\rho = 0.5$ and $SD = 0.75$. Thus, $\mathcal{R}_c = 0.2585 < 1$. Therefore, we expect that the solution curves of the model tend to the COVID-19 free equilibrium point $P_0 = (1,\ 0,\ 0,\ 0,\ 0)$. This is evident in Figure 3; the numerical solutions eventually reach P_0 for different initial conditions. Accordingly, COVID-19 diminishes.

Experiment 2: In this experiment, we increased the value of the parameter ρ and decreased the values of the parameters ε and SD. That is to say, the control measures of lockdown, social distancing and random diagnostic testing were reduced. We assume the parameters of Model (4.2) have the following values: $\mu = 0.04$, $\eta = 1250$, $\gamma = 0.167$, $\beta_1 = 0.0554 \times 10^{-4}$, $\beta_2 = 1.0596 \times 10^{-4}$, $\varepsilon = 0.10$, $\theta = 0.54$, $\delta = 3.2772 \times 10^{-1}$, $d = 2.3724 \times 10^{-1}$, $\rho = 0.85$ and $SD = 0.30$. Therefore, $\mathcal{R}_c = 2.1639 > 1$. Hence, we expect the solution curves of the model to approach the COVID-19 endemic equilibrium point P_1. This is displayed in Figure 4; the numerical solutions eventually tend to $P_1 = (0.4621,\ 0.1039,\ 0.0255,\ 0.0132,\ 0.3170)$ for different initial conditions. Consequently, COVID-19 remains at a specific percentage.

We conclude from the experiments that the numerical results are in good agreement with the qualitative results.

4.3. Sensitivity analysis for $\mathcal{R}_c$

To determine which parameters influence the spread of COVID-19, we investigated the sensitivity of the control reproduction number for Model (2.1). The sensitivity of $\mathcal{R}_c$ was examined analytically by evaluating $\partial\mathcal{R}_c/\partial\mathcal{P}$, where $\mathcal{P} = (\eta, \beta_1, \beta_2, \rho, SD, \gamma, \delta, \varepsilon, \theta, d, \mu)$. The changes in $\mathcal{R}_c$ corresponding to

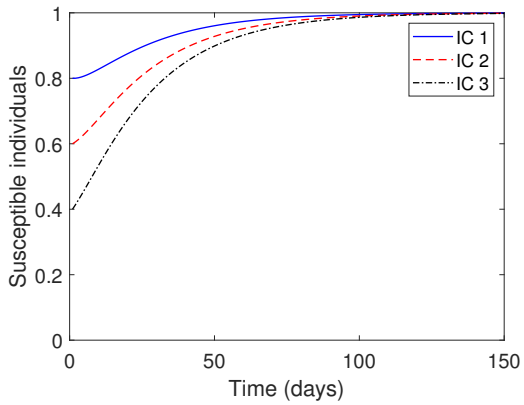

(a) Susceptible compartment

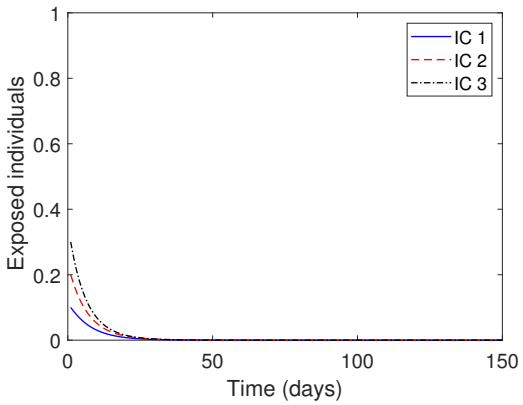

(b) Exposed compartment

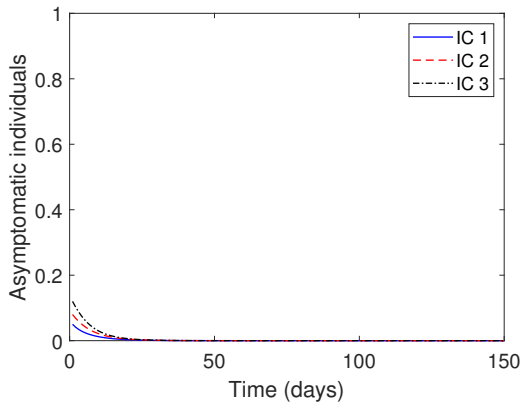

(c) Asymptomatic compartment

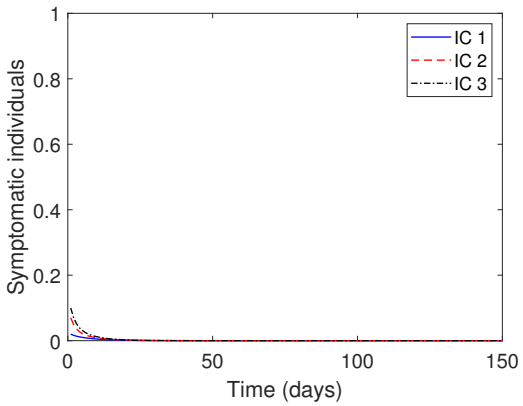

(d) Symptomatic compartment

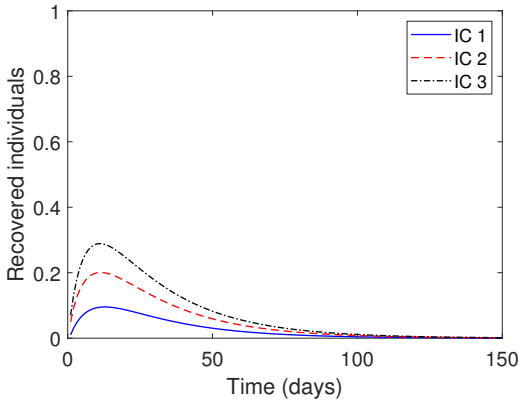

(e) Recovered compartment

Figure 3. Numerical solution of Model (2.1) with different initial conditions for $\mathcal{R}_c < 1$.

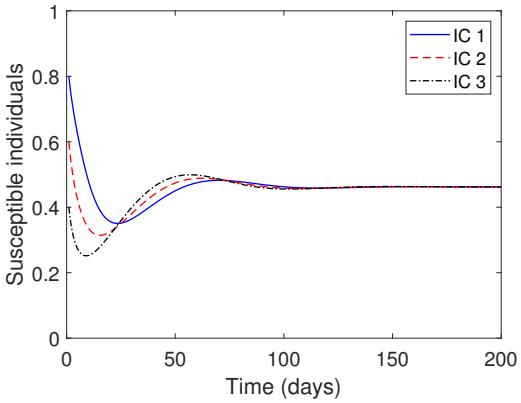

(a) Susceptible compartment

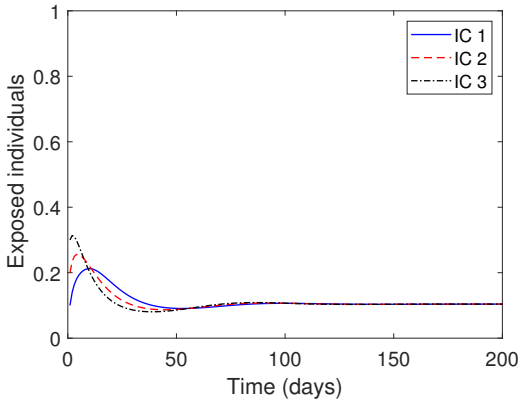

(b) Exposed compartment

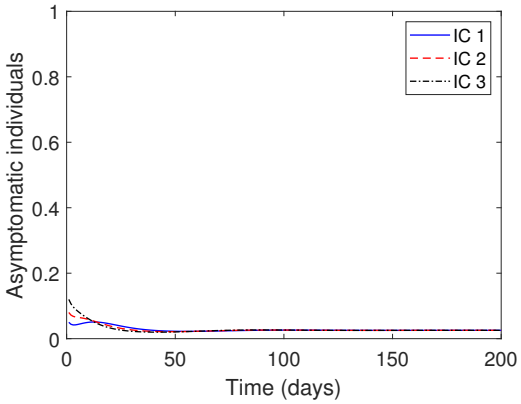

(c) Asymptomatic compartment

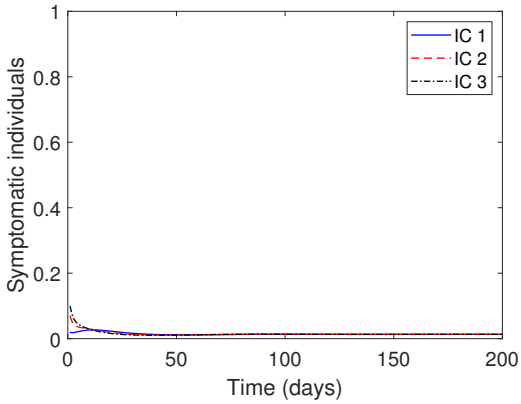

(d) Symptomatic compartment

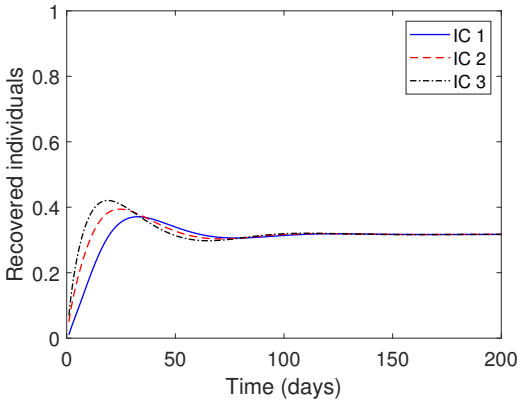

(e) Recovered compartment

Figure 4. Numerical solution of Model (2.1) with different initial conditions for $\mathcal{R}_c > 1$.

one parameter at a time are as follows:

$$
\begin{aligned}
\frac{\partial \mathcal{R}_c}{\partial \varepsilon} &= \frac{-\eta\gamma\rho(1-SD)\beta_2\theta}{\mu(\gamma+\mu)(\delta+\mu)} < 0,\\
\frac{\partial \mathcal{R}_c}{\partial \beta_1} &= \frac{\eta\gamma\rho(1-SD)(1-\theta)}{\mu(\gamma+\mu)(\delta+d+\mu)} > 0,\\
\frac{\partial \mathcal{R}_c}{\partial \beta_2} &= \frac{\eta\gamma\rho(1-SD)\theta(1-\varepsilon)}{\mu(\gamma+\mu)(\delta+\mu)} > 0,\\
\frac{\partial \mathcal{R}_c}{\partial d} &= \frac{-\eta\gamma\rho(1-SD)\beta_1(1-\theta)}{\mu(\gamma+\mu)(\delta+d+\mu)^2} < 0,\\
\frac{\partial \mathcal{R}_c}{\partial SD} &= \frac{-\eta\gamma\rho}{\mu(\gamma+\mu)}\left[\frac{\beta_1(1-\theta)}{(\delta+d+\mu)} + \frac{\beta_2\theta(1-\varepsilon)}{(\delta+\mu)}\right] < 0,\\
\frac{\partial \mathcal{R}_c}{\partial \eta} &= \frac{\gamma\rho(1-SD)}{\mu(\gamma+\mu)}\left[\frac{\beta_1(1-\theta)}{(\delta+d+\mu)} + \frac{\beta_2\theta(1-\varepsilon)}{(\delta+\mu)}\right] > 0,\\
\frac{\partial \mathcal{R}_c}{\partial \gamma} &= \frac{\eta\rho(1-SD)}{(\gamma+\mu)^2}\left[\frac{\beta_1(1-\theta)}{(\delta+d+\mu)} + \frac{\beta_2\theta(1-\varepsilon)}{(\delta+\mu)}\right] > 0,\\
\frac{\partial \mathcal{R}_c}{\partial \rho} &= \frac{\eta\gamma(1-SD)}{\mu(\gamma+\mu)}\left[\frac{\beta_1(1-\theta)}{(\delta+d+\mu)} + \frac{\beta_2\theta(1-\varepsilon)}{(\delta+\mu)}\right] > 0,\\
\frac{\partial \mathcal{R}_c}{\partial \delta} &= \frac{-\eta\gamma\rho(1-SD)}{\mu(\gamma+\mu)}\left[\frac{\beta_1(1-\theta)}{(\delta+d+\mu)^2} + \frac{\beta_2\theta(1-\varepsilon)}{(\delta+\mu)^2}\right] < 0,\\
\frac{\partial \mathcal{R}_c}{\partial \theta} &= \frac{\eta\gamma\rho(1-SD)}{\mu(\gamma+\mu)}\left[\frac{\beta_2(1-\varepsilon)}{(\delta+\mu)} - \frac{\beta_1}{(\delta+d+\mu)}\right]\\
&= \frac{\eta\gamma\rho(1-SD)\beta_2}{\mu(\gamma+\mu)(\delta+\mu)}(1-\omega) > 0 \quad \text{when } \omega < 1 \quad (< 0 \text{ when } \omega > 1),\\
\frac{\partial \mathcal{R}_c}{\partial \mu} &= \frac{-\eta\gamma\rho(1-SD)(\gamma+2\mu)}{\mu^2(\gamma+\mu)^2}\left[\frac{\beta_1(1-\theta)}{(\delta+d+\mu)} + \frac{\beta_2\theta(1-\varepsilon)}{(\delta+\mu)}\right]\\
&\quad - \frac{\eta\gamma\rho(1-SD)}{\mu(\gamma+\mu)}\left[\frac{\beta_1(1-\theta)}{(\delta+d+\mu)^2} + \frac{\beta_2\theta(1-\varepsilon)}{(\delta+\mu)^2}\right] < 0,
\end{aligned}
\tag{4.3}
$$

where $\omega = \varepsilon + (\beta_1(\delta+\mu)/\beta_2(\delta+d+\mu))$. From Eq (4.3), we see that an increase in ε, SD, δ, d or μ leads to a decrease in $\mathcal{R}_c$. Conversely, an increase in β_1, β_2, ρ, γ or η leads to an increase in $\mathcal{R}_c$. Finally, the sensitivity of $\mathcal{R}_c$ with respect to θ depends on the value of ω. If $\omega > 1$, then $\mathcal{R}_c$ decreases, and if $\omega < 1$, $\mathcal{R}_c$ increases. Figure 5 illustrates these results.

The normalized sensitivity index (elasticity) of $\mathcal{R}_c$ with respect to the model parameters $\mathcal{P}$ is defined as follows [47]:

$$
\Gamma_{\mathcal{R}_c}^{\mathcal{P}} = \frac{\partial \mathcal{R}_c}{\partial \mathcal{P}} \frac{\mathcal{P}}{\mathcal{R}_c}. \tag{4.4}
$$

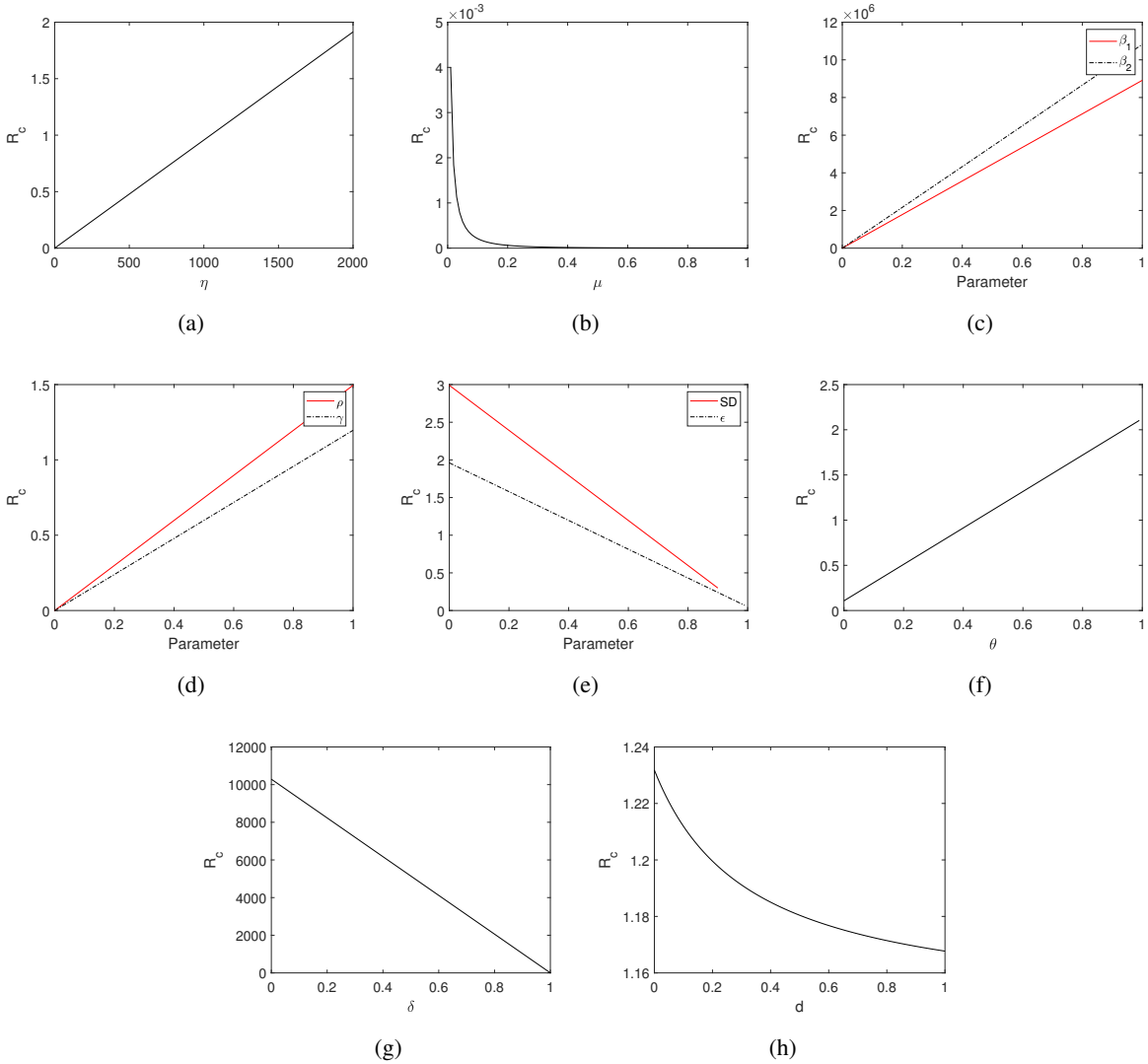

Figure 5. Sensitivity of $\mathcal{R}_c$ with respect to the parameters of Model (2.1).

By applying the formula in Eq (4.4), we get

$$
\begin{aligned}
\Gamma^{\eta}_{\mathcal{R}_c} &= 1,\\
\Gamma^{\rho}_{\mathcal{R}_c} &= 1,\\
\Gamma^{\gamma}_{\mathcal{R}_c} &= \frac{\mu}{\gamma+\mu},\\
\Gamma^{SD}_{\mathcal{R}_c} &= \frac{-SD}{1-SD},\\
\Gamma^{\theta}_{\mathcal{R}_c} &= \frac{\beta_2\theta(1-\varepsilon)(\delta+d+\mu)-\beta_1\theta(\delta+\mu)}{\beta_2\theta(1-\varepsilon)(\delta+d+\mu)+\beta_1(1-\theta)(\delta+\mu)},\\
\Gamma^{\beta_1}_{\mathcal{R}_c} &= \frac{\beta_1(1-\theta)(\delta+\mu)}{\beta_1(1-\theta)(\delta+\mu)+\beta_2\theta(1-\varepsilon)(\delta+d+\mu)},\\
\Gamma^{\beta_2}_{\mathcal{R}_c} &= \frac{\beta_2\theta(1-\varepsilon)(\delta+d+\mu)}{\beta_1(1-\theta)(\delta+\mu)+\beta_2\theta(1-\varepsilon)(\delta+d+\mu)},\\
\Gamma^{\varepsilon}_{\mathcal{R}_c} &= \frac{-\beta_2\varepsilon\theta(\delta+d+\mu)}{\beta_1(1-\theta)(\delta+\mu)+\beta_2\theta(1-\varepsilon)(\delta+d+\mu)},\\
\Gamma^{d}_{\mathcal{R}_c} &= \frac{-d\beta_1(1-\theta)(\delta+\mu)}{\beta_1(1-\theta)(\delta+\mu)(\delta+d+\mu)+\beta_2\theta(1-\varepsilon)(\delta+d+\mu)^2},\\
\Gamma^{\delta}_{\mathcal{R}_c} &= \frac{-\delta}{(\delta+\mu)(\delta+d+\mu)}\left[\frac{\beta_1(1-\theta)(\delta+\mu)^2+\beta_2\theta(1-\varepsilon)(\delta+d+\mu)^2}{\beta_1(1-\theta)(\delta+\mu)+\beta_2\theta(1-\varepsilon)(\delta+d+\mu)}\right],\\
\Gamma^{\mu}_{\mathcal{R}_c} &= \frac{-(\gamma+2\mu)}{(\gamma+\mu)}-\frac{\mu}{(\delta+\mu)(\delta+d+\mu)}\left[\frac{\beta_1(1-\theta)(\delta+\mu)^2+\beta_2\theta(1-\varepsilon)(\delta+d+\mu)^2}{\beta_1(1-\theta)(\delta+\mu)+\beta_2\theta(1-\varepsilon)(\delta+d+\mu)}\right].
\end{aligned}
$$

Table 3. Sensitivity index for $\mathcal{R}_c$ with respect to the parameters $\mathcal{P}$ of Model (2.1).

Parameter $\mathcal{P}$	Value	Sensitivity index $\Gamma^{\mathcal{P}}_{\mathcal{R}_c}$
η	1250	1
β_1	0.0554×10^{-7}	0.0413
β_2	1.0596×10^{-7}	0.9587
γ	0.167	0.0002
θ	0.54	0.9103
δ	3.2772×10^{-1}	−0.9826
d	2.3724×10^{-1}	−0.0173
μ	3.653×10^{-5}	−1.0003
ρ	0.80	1
ε	0.40	−0.6391
SD	0.10	−0.1111
	0.30	−0.4286
	0.50	−1
	0.70	−2.3333
	0.90	−9
	0.99	−99

Table 3 exhibits the elasticity of $\mathcal{R}_c$ with respect to the model parameters. The parameter values were taken from Table 1, in addition to $\rho = 0.80$, $SD = 0.60$ and $\varepsilon = 0.40$. Any positive value for the elasticity in Table 3 means that the contribution of the parameter to $\mathcal{R}_c$ is to increase its value. For instance, $\Gamma_{\mathcal{R}_c}^{\beta_2} = 0.9587$ means that an increase in β_2 by 1% will increase $\mathcal{R}_c$ by 0.9587%. On the contrary, any negative value for the elasticity means that the contribution of the parameter to $\mathcal{R}_c$ is to decrease its value. For example, $\Gamma_{\mathcal{R}_c}^{\varepsilon} = -0.6391$ means that an increase in ε by 1% will decrease $\mathcal{R}_c$ by 0.6391%. We notice that the most sensitive parameters are β_2, ρ, SD and ε. Therefore, the increase in imposing social distancing and lockdown measures and detecting asymptomatic individuals through random diagnostic testing reduces the spread of the disease.

4.4. Different scenarios for control strategies

Model (2.1) examines some of the policies that have been applied in Saudi Arabia to control COVID-19, namely, the effectiveness of random diagnostic testing on the asymptomatic class (ε), lockdown (ρ) and social distancing (SD). We executed several scenarios to investigate the impact of these policies by simulating Model (2.1) for infected cases. Figure 2 shows the actual data in Saudi Arabia and the fitting curve for Model (2.1) for infected cases from March 12, 2020 to September 23, 2020. We solve Model (2.1) numerically with the following initial values: $S(0) = 34813577$, $E(0) = 150$, $I_a(0) = 95$, $I_s(0) = 44$, $R(0) = 1$ and the parameter values given in Table 1. The parameters ε, ρ and SD took different values for each scenario. We describe different scenarios in Table 4. For the fitting values of ρ and SD, refer to Table 2.

Table 4. Different scenarios for Model (2.1).

Scenario	ε	ρ	SD
1^{st}	Different values	Fitting values	Fitting values
2^{nd}	Different values	No lockdown ($\rho = 1$)	No social distancing ($SD = 0$)
3^{rd}	Different values	Different values	Fitting values
4^{th}	Different values	Fitting values	Different values
5^{th}	Different values	0.85	Different values
6^{th}	Different values	0.75	Different values
7^{th}	Different values for three time periods	Fitting values	Fitting values

Table 5. Results of 1^{st} scenario.

ρ	SD	ε	Peak (day)	Cases	Percentage Change
Fitting values	Fitting values	0.01	122	52,010	−13.07%
		0.02	122	45,140	−24.55%
		0.03	122	39,120	−34.61%
		0.04	122	33,830	−43.45%
		0.10	121	13,770	−76.98%
		0.20	68	4,159	−93.04%
		0.30	58	1,556	−97.39%
		0.40	37	705	−98.82%

The results of applying the scenarios (1^{st} – 7^{th}) are summarized in Tables 5–11 and illustrated in Figures 6–12. We compared the scenarios with the peak value of the infected cases in the fitting of Model (2.1), that is, 59, 830, which occured on Day 123.

The 1^{st} scenario examines the impact of detecting asymptomatic individuals by applying random diagnostic testing in Saudi Arabia. At the same time, the lockdown and social distancing are kept as the fitting values. Figure 6 illustrates that the peak of infected cases decreases with increasing ε. For instance, when detecting only 2% of the asymptomatic individuals ($\varepsilon = 0.02$) by random diagnostic testing, the cases will reach 45,140 on Day 122. Compared with actual data, the number of cases decreased by 24.55% (see Table 5). This indicates the importance of applying the random diagnostic testing to find asymptomatic individuals and reduce the cases.

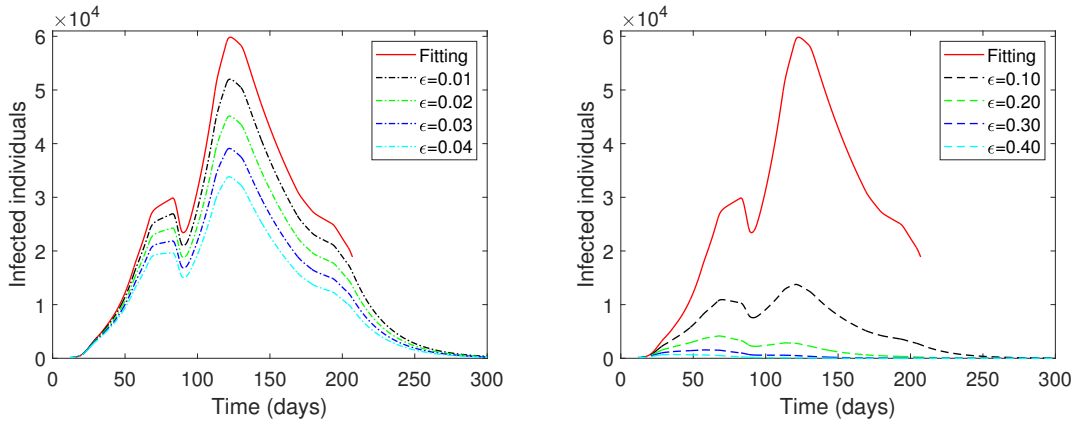

Figure 6. Numerical solution of Model (2.1) for infected compartments vs. time for the 1^{st} scenario: different values for ε, and ρ and SD are the same as the fitting values.

Table 6. Results of 2^{nd} scenario.

ρ	SD	ε	Peak (day)	Cases	Percentage Change
1	0	0.10	53	4,728,000	+7802.39%
		0.20	57	4,420,000	+7287.60%
		0.30	62	4,057,000	+6680.88%
		0.40	69	3,607,000	+5928.75%
		0.50	79	3,042,000	+4984.41%
		0.60	97	2,332,000	+3797.71%
		0.70	133	1,431,000	+2291.78%
		0.80	266	391,700	+554.68%

The 2^{nd} scenario was applied to determine whether it is possible to rely only on detecting asymptomatic individuals through random diagnostic testing without imposing social distancing and a lockdown. Figure 7 shows that the infected cases will far surpass the actual data. For example, if the detection of asymptomatic cases reaches 60% ($\varepsilon = 0.60$), the peak of cases will be 2, 332, 000 on Day 97 (see Table 6). That is an increase of 3797.71% relative to the peak value of the actual data. We

concluded that detecting asymptomatic individuals is insufficient without imposing social distancing and lockdown.

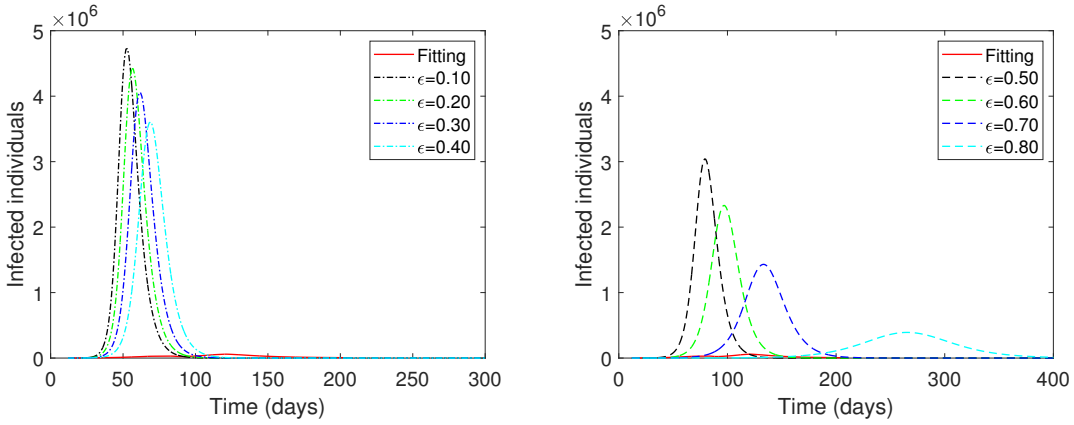

Figure 7. Numerical solution of Model (2.1) for infected compartments vs. time for 2^{nd} scenario: different values for ε, $\rho = 1$ and $SD = 0$.

Table 7. Results of 3^{rd} scenario.

ρ	SD	ε	Peak (day)	Cases	Percentage Change
1	Fitting values	0.10	84	1,163,000	+1843.84%
		0.20	112	630,200	+953.31%
		0.30	115	195,700	+227.09%
		0.40	113	27,360	−54.27%
0.85	Fitting values	0.10	113	454,000	+658.81%
		0.20	115	127,900	+113.77%
		0.30	113	22,410	−62.54%
		0.40	77-83	4,208	−92.96%
0.75	Fitting values	0.10	115	110,600	+84.85%
		0.20	113	23,550	−60.63%
		0.30	83	5,273	−91.18%
		0.40	68	1,514	−97.46%
0.55	Fitting values	0.10	70	2,882	−95.18%
		0.20	68	1,175	−98.03%
		0.30	58	474	−99.20%
		0.40	30	244	−99.59%

The 3^{rd} scenario analyzes four different values for the level of lockdown ($\rho = 1,\ 0.85,\ 0.75,\ 0.55$) the values for social distancing were kept as the fitting values. When $\rho = 1$, there is no lockdown implementation. The remaining values of ρ correspond to the lockdown level undertaken by Saudi Arabia in Phase 1, Phase 2 and Phase 4, respectively [37].

Figure 8 shows that increasing the lockdown level leads to a decrease in the infected cases. Note

that increasing the lockdown level means decreasing the value of ρ. Moreover, increasing the lockdown level requires a smaller value for detecting asymptomatic individuals through random diagnostic testing to reach case numbers lower than the actual data. To explain further, when the lockdown level is equal to 1, 0.85, 0.75 or 0.55, we need to apply a 40, 30, 20 or 10% level of random diagnostic testing, respectively, to detect the asymptomatic individuals (see Table 7).

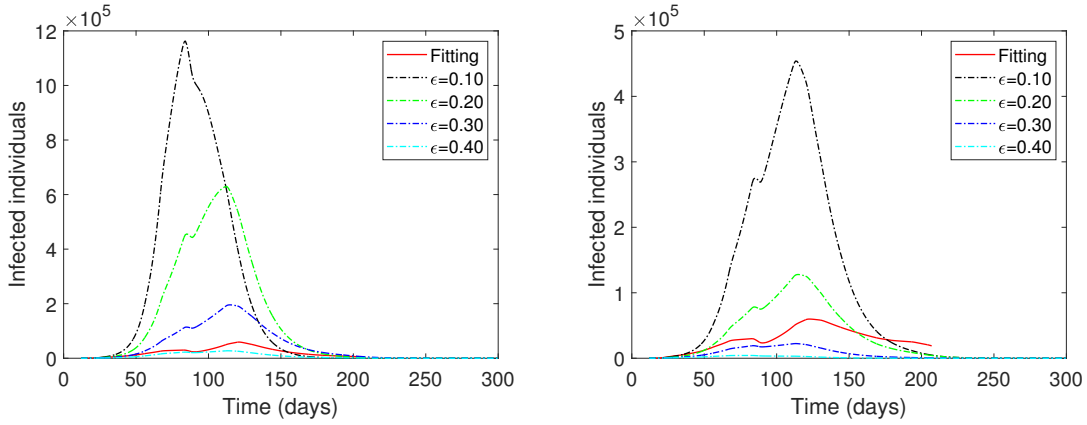

(a) $\rho = 1$ (b) $\rho = 0.85$

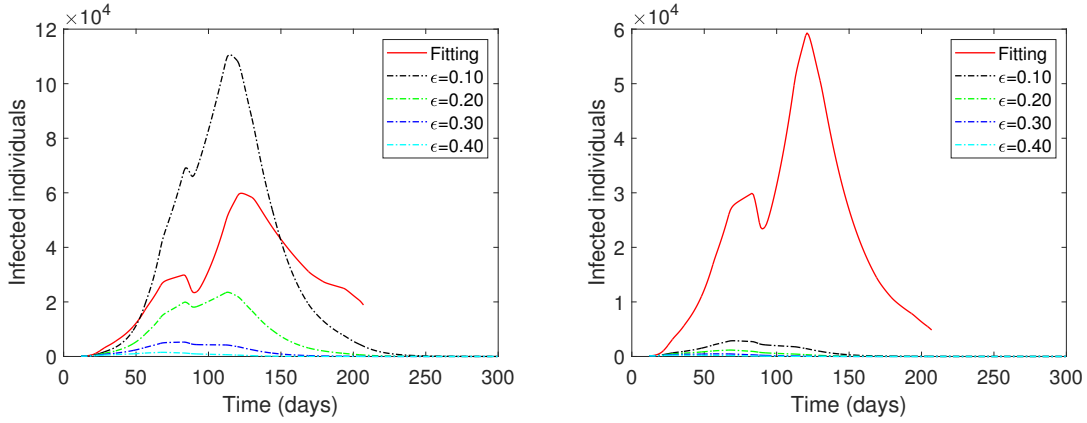

(c) $\rho = 0.75$ (d) $\rho = 0.55$

Figure 8. Numerical solution of Model (2.1) for infected compartments vs. time for 3^{rd} scenario: different values for ε and ρ; SD is the same as the fitting values.

The 4^{th} scenario investigates the impact of social distancing while keeping the value of ρ equal to the fitting values. Figure 9 illustrates that increasing the application of social distancing delays peak days; however, only when $SD = 0.70$ and $\varepsilon = 0.40$ does the cases reach a value that is lower than the actual data by 51.81%, i.e., 28, 830 (see Table 8).

The 5^{th} and 6^{th} scenarios examine the impact of imposing a lockdown at low levels and relying on social distancing and random diagnostic testing. We let $\rho = 0.85$ and 0.75 for the 5^{th} and 6^{th} scenarios, respectively. Figures 10 and 11 show that it is possible to reach a lower number of infected cases than in the actual data if $SD = 0.70$, where $\varepsilon = 0.40$ for the case where $\rho = 0.85$ (see Table 9), and $\varepsilon = 0.30$ for the case where $\rho = 0.75$ (see Table 10). This indicates that enforcing low lockdown levels is effective with a high level of social distancing implementation and 30% or more of the detection of

asymptomatic individuals through random diagnostic testing.

Table 8. Results of 4^{th} scenario.

ρ	SD	ε	Peak (day)	Cases	Percentage Change
Fitting values	0.40	0.10	124	2,314,000	+3767.62%
		0.20	138, 139	2,035,000	+3301.30%
		0.30	160	1,764,000	+2848.35%
		0.40	194	1,441,000	+2308.49%
Fitting values	0.50	0.10	150	1,874,000	+3032.21%
		0.20	171	1,629,000	+2622.71%
		0.30	203	1,434,000	+2296.79%
		0.40	247	1,121,000	+1773.64%
Fitting values	0.60	0.10	198	1,439,000	+2305.15%
		0.20	229	1,271,000	+2024.35%
		0.30	279	902,300	+1408.11%
		0.40	377	506,400	+746.39%
Fitting values	0.70	0.10	302	776,200	+1197.34%
		0.20	387	480,900	+703.77%
		0.30	572	213,800	+257.34%
		0.40	1402, 1408	28,830	−51.81%

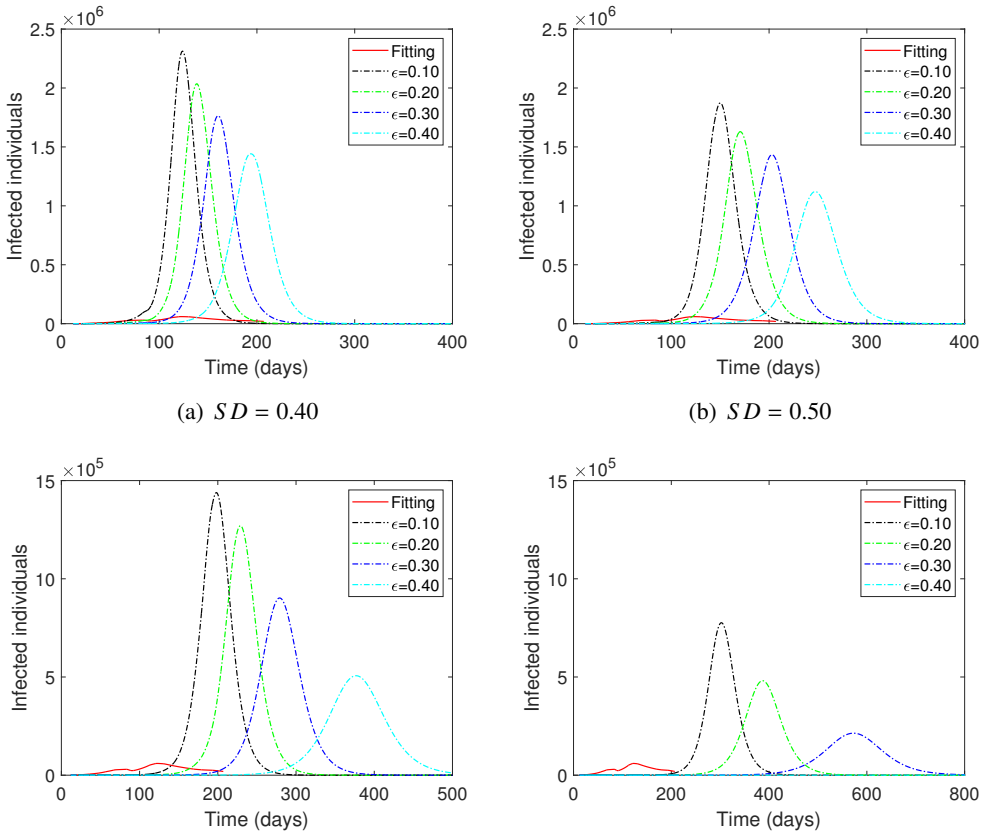

(a) $SD = 0.40$ (b) $SD = 0.50$

(c) $SD = 0.60$ (d) $SD = 0.70$

Figure 9. Numerical solution of Model (2.1) for infected compartments vs. time for 4^{th} scenario: different values for ε and SD; ρ is the same as the fitting values.

Table 9. Results of 5^{th} scenario.

ρ	SD	ε	Peak (day)	Cases	Percentage Change
0.85	0.40	0.10	88	2,674,000	+4369.33%
		0.20	98	2,284,000	+3717.48%
		0.30	114	1,847,000	+2987.08%
		0.40	138	1,357,000	+2168.09%
0.85	0.50	0.10	106	2,052,000	+3329.72%
		0.20	121, 122	1,666,000	+2684.56%
		0.30	145	1,247,000	+1984.24%
		0.40	185, 186	801,700	+1239.96%
0.85	0.60	0.10	141	1,310,000	+2089.54%
		0.20	168, 169	957,200	+1499.87%
		0.30	216	599,300	+901.67%
		0.40	320	265,700	+344.09%
0.85	0.70	0.10	240	488,600	+716.64%
		0.20	331, 332	246,000	+311.16%
		0.30	600	60,790	+1.60%
		0.40	12	139	−99.76%

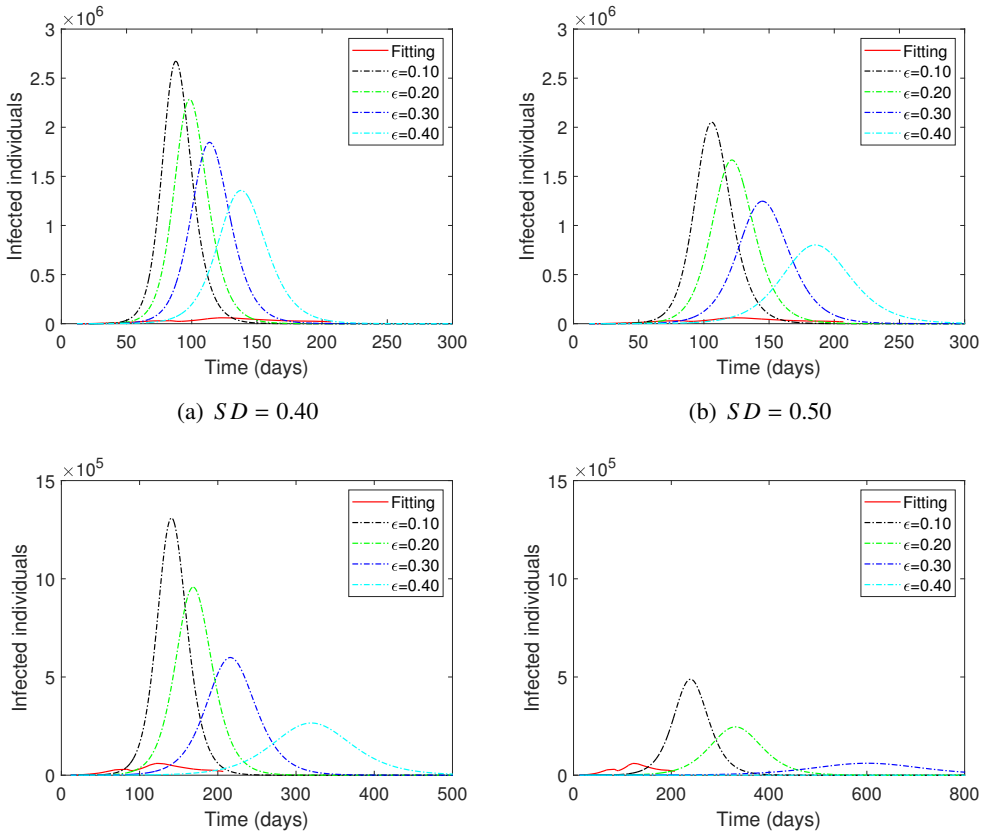

(a) $SD = 0.40$ (b) $SD = 0.50$

(c) $SD = 0.60$ (d) $SD = 0.70$

Figure 10. Numerical solution of Model (2.1) for infected compartments vs. time for 5^{th} scenario: different values for ε and SD, while $\rho = 0.85$.

Table 10. Results of 6^{th} scenario.

ρ	SD	ε	Peak (day)	Cases	Percentage Change
0.75	0.40	0.10	100	2,246,000	+3653.97%
		0.20	113	1,859,000	+3007.14%
		0.30	133, 134	1,430,000	+2290.11%
		0.40	167	967,500	+1517.08%
0.75	0.50	0.10	123	1,630,000	+2624.39%
		0.20	144	1,259,000	+2004.30%
		0.30	178	867,000	+1349.11%
		0.40	242	475,400	+694.58%
0.75	0.60	0.10	172	924,900	+1445.88%
		0.20	214, 215	608,800	+917.55%
		0.30	297	310,600	+419.13%
		0.40	550	75,830	+26.74%
0.75	0.70	0.10	344	226,300	+278.23%
		0.20	585-588	64,690	+8.12%
		0.30	12	139	−99.76%
		0.40	12	139	−99.76%

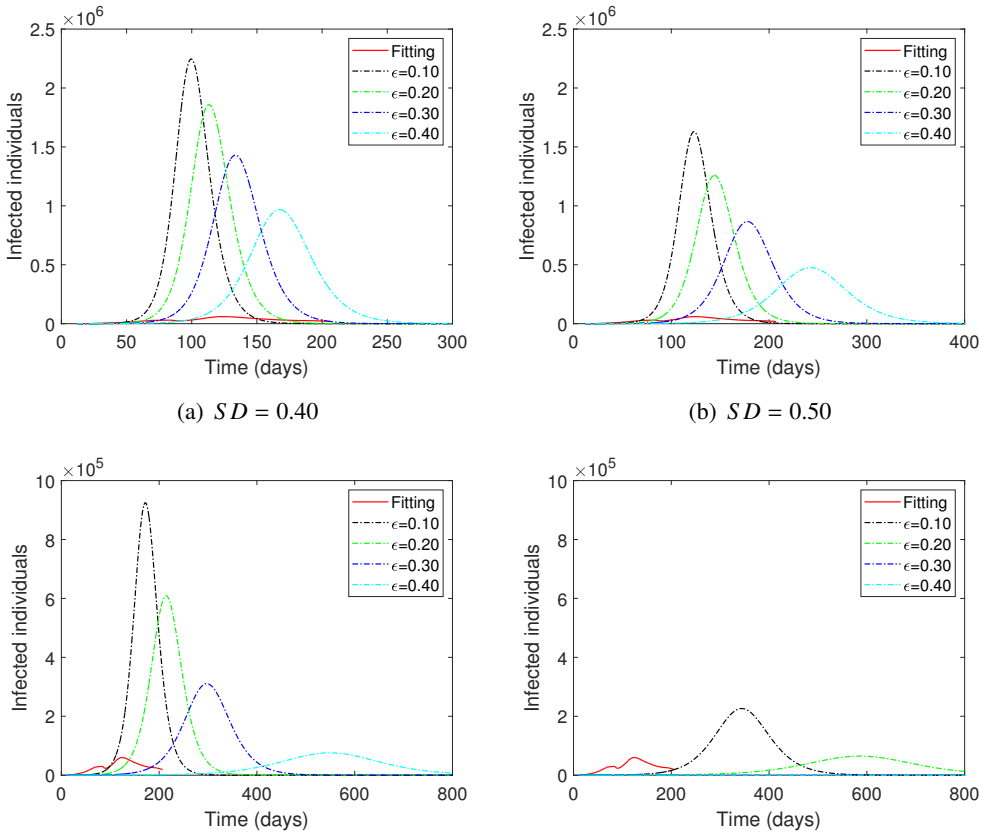

(a) $SD = 0.40$ (b) $SD = 0.50$

(c) $SD = 0.60$ (d) $SD = 0.70$

Figure 11. Numerical solution of Model (2.1) for infected compartments vs. time for 6^{th} scenario: different values for ε and SD, while $\rho = 0.75$.

Table 11. Results of 7^{th} scenario.

Event	ε_1	ε_2	ε_3	Peak (day)	Cases	Percentage Change
I	0.10	0	0	123	38,480	−35.68%
II	0.10	0.10	0	124	20,890	−65.08%
III	0	0.10	0.10	121	21,920	−63.36%
IV	0.20	0	0	124	23,650	−60.47%
V	0.20	0.20	0	125	6,539	−89.07%
VI	0	0.20	0.20	68	11,470	−80.82%
VII	0.10	0.20	0	125	10,870	−81.83%
VIII	0.10	0.20	0.10	121	7,132	−88.07%
IX	0.20	0.10	0	124, 125	12,680	−78.80%
X	0.20	0.10	0.10	121	8,326	−86.08%
XI	0	0.20	0.10	121	11,480	−80.81%

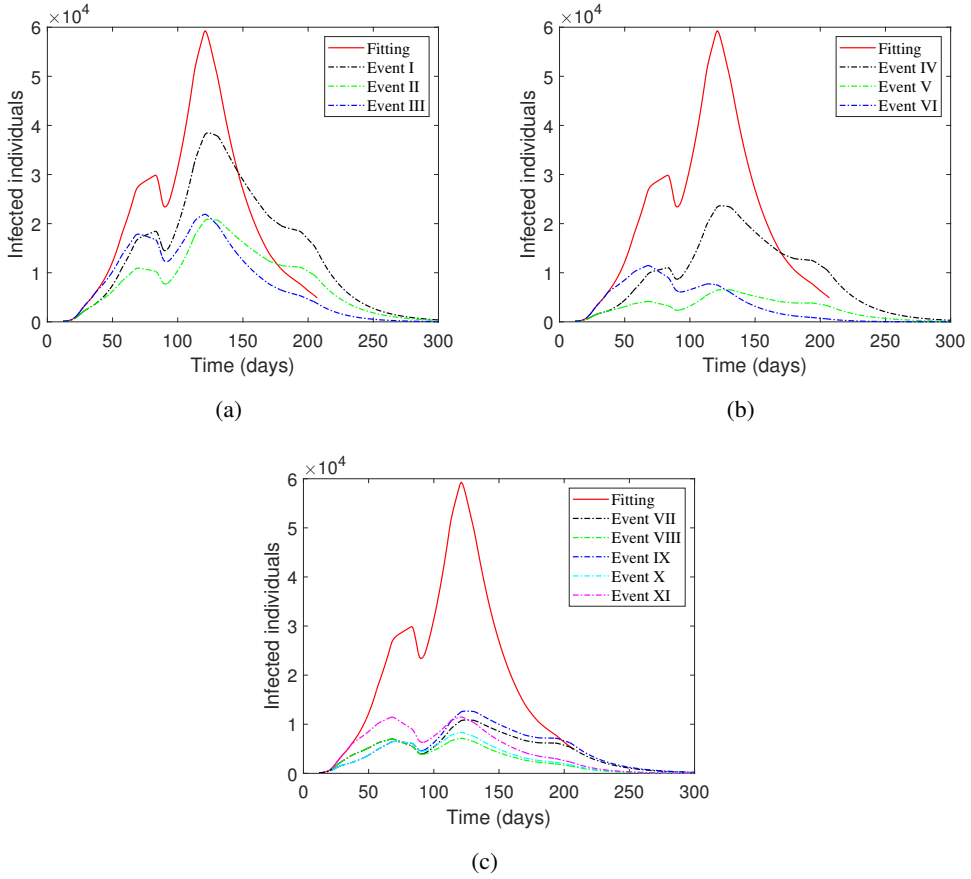

Figure 12. Numerical solution of Model (2.1) for infected compartments vs. time for 7^{th} scenario: different values for ε, where ε is divided into ε_1, ε_2 and ε_3. The value of SD and ρ are the same as the fitting values.

The 7^{th} scenario was designed to determine the effect of different values of ε through the phases. We assume that the value of ε is ε_1 in Phase 1 to Phase 2, ε_2 in Phase 3 to Phase 5 and ε_3 in Phase 6 to Phase 7 (see Table 11). Figure 12(a) and (b) show that performing random diagnostic tests in the middle phases (Phase 3–5) and the beginning phases (Phase 1 and 2), rather than the last phases (Phase

6 and 7), gives better results. Furthermore, applying the tests in all phases reduces the number of cases, as seen in Figure 12(c).

We conclude from the analysis of the 1^{st} to the 6^{th} scenarios that applying random diagnostic testing alone is inadequate without imposing social distancing and lockdown. The importance of using random diagnostic testing to find asymptomatic individuals is apparent when lockdown and social distancing measures are enforced; only then does the number of cases decline. An increase in the level of lockdown decreases the required percentage of random diagnostic tests to lower the number of cases. However, an increase in social distancing does not have the same effect as a lockdown; a high percentage of random diagnostic tests is needed to reduce the number of cases. On the other hand, implementation of lower levels of lockdown is possible only when a high level of social distancing and a high percentage of random diagnostic tests are imposed.

As for the 7^{th} scenario, we deduce that performing the random diagnostic tests in all phases is effective in lowering the number of cases. However, applying the random diagnostic tests in the early and middle phases is sufficient to reduce the cost of conducting these tests.

5. Conclusions

This study was purposed to develop a mathematical model to examine the impact of random diagnostic testing on COVID-19 patients in the presence of a lockdown and social distancing in Saudi Arabia. Qualitative and numerical analyses were applied to the model. The model was well posed and had two equilibrium points. The COVID-19 free equilibrium existed and was locally and globally asymptotically stable if $\mathcal{R}_c < 1$. Conversely, the COVID-19 endemic equilibrium existed and was locally and globally asymptotically stable if $\mathcal{R}_c > 1$.

The model was validated by using the data from the COVID-19 dashboard of the Saudi Ministry of Health spanning March 12, 2020 to September 23, 2020. In addition, the numerical experiments performed using the model showed the consistency of the numerical solutions with the qualitative analysis.

Furthermore, the sensitivity analysis for $\mathcal{R}_c$ revealed that the most influential parameter in terms of increasing $\mathcal{R}_c$ was the transmission rate due to contact with asymptomatic individuals (β_2). However, the control parameters, i.e., the lockdown (ρ), social distancing (SD) and the effectiveness of random diagnostic testing for asymptomatic individuals (ε), played a significant role in decreasing $\mathcal{R}_c$. Finally, we analyzed different scenarios numerically for the control strategies applied in Saudi Arabia.

We concluded that applying random diagnostic testing to detect asymptomatic individuals in the presence of a lockdown and social distancing significantly reduced the cases. On the other hand, it was impossible to rely on random diagnostic testing without imposing a lockdown and social distancing. Moreover, implementing a lockdown at low levels required increased social distancing levels and a high percentage of random diagnostic testing.

Conflict of interest

The authors declare that there is no conflict of interest.

References

1. WHO Director-General's opening remarks at the media briefing on COVID-19 - 11 March 2020, 2020. Available from: https://www.who.int/director-general/speeches/detail.

2. Weekly epidemiological update on COVID-19 - 28 December 2021, 2021. Available from: https://www.who.int/publications/m/item/weekly-epidemiological-update-on-covid-19–28-december-2021.

3. Y. Wang, Y. Wang, Y. Chen, Q. Qin, Unique epidemiological and clinical features of the emerging 2019 novel coronavirus pneumonia (COVID-19) implicate special control measures, *J. Med. Virol.*, **92** (2020), 568–576. https://doi.org/10.1002/jmv.25748

4. Z. Gao, Y. Xu, C. Sun, X. Wang, Y. Guo, S. Qiu, et al., A systematic review of asymptomatic infections with COVID-19. *J. Microbiol. Immunol. Infect.*, **54** (2021), 12–16. https://doi.org/10.1016/j.jmii.2020.05.001

5. Y. Bai, L. Yao, T. Wei, F. Tian, D. Jin, L. Chen, et al., Presumed asymptomatic carrier transmission of COVID-19, *Jama*, **323** (2020), 1406–1407. https://doi.org/10.1001/jama.2020.2565

6. R. Li, S. Pei, B. Chen, Y. Song, T. Zhang, W. Yang, et al., Substantial undocumented infection facilitates the rapid dissemination of novel coronavirus (SARS-CoV-2), *Science*, **368** (2020), 489–493. https://doi.org/10.1126/science.abb3221

7. G. Kim, M. Kim, S. Ra, J. Lee, S. Bae, J. Jung, et al., Clinical characteristics of asymptomatic and symptomatic patients with mild COVID-19, *Clin. Microbiol. Infect.*, **26** (2020), 948.e1–948.e3. https://doi.org/10.1016/j.cmi.2020.04.040

8. J. M. AlJishi, A. H. Alhajjaj, F. L. Alkhabbaz, T. H. AlAbduljabar, A. Alsaif, H. Alsaif, et al., Clinical characteristics of asymptomatic and symptomatic COVID-19 patients in the eastern province of Saudi Arabia, *J. Infect. Public Health*, **14** (2021), 6–11. https://doi.org/10.1016/j.jiph.2020.11.002

9. Y. M. Alsofayan, S. M. Althunayyan, A. A. Khan, A. M. Hakawi, A. M. Assiri, Clinical characteristics of COVID-19 in Saudi Arabia: A national retrospective study, *J. Infect. Public Health*, **13** (2020), 920–925. https://doi.org/10.1016/j.jiph.2020.05.026

10. F. S. Alshammari, A mathematical model to investigate the transmission of COVID-19 in the kingdom of Saudi Arabia, *Comput. Math. Methods. Med.*, **2020** (2020), 1–13. https://doi.org/10.1155/2020/9136157

11. I. Ahmed, G. U. Modu, A. Yusuf, P. Kumam, I. Yusuf, A mathematical model of Coronavirus Disease (COVID-19) containing asymptomatic and symptomatic classes, *Results Phys.*, **21** (2021), 103776. https://doi.org/10.1016/j.rinp.2020.103776

12. N. Anggriani, M. Z. Ndii, R. Amelia, W. Suryaningrat, M. A. A. Pratama, A mathematical COVID-19 model considering asymptomatic and symptomatic classes with waning immunity, *Alexandria Eng. J.*, **61** (2022), 113–124. https://doi.org/10.1016/j.aej.2021.04.104

13. E. Alzahrani, M. El-Dessoky, D. Baleanu, Mathematical modeling and analysis of the novel Coronavirus using Atangana–Baleanu derivative, *Results Phys.*, **25** (2021), 104240. https://doi.org/10.1016/j.rinp.2021.104240

14. M. S. Alqarni, M. Alghamdi, T. Muhammad, A. S. Alshomrani, M. A. Khan, Mathematical modeling for novel coronavirus (COVID-19) and control, *Numer. Methods Partial. Differ. Equ.*, (2020), 1–17. https://doi.org/10.1002/num.22695

15. T. Sun, D. Weng, Estimating the effects of asymptomatic and imported patients on COVID-19 epidemic using mathematical modeling, *J. Med. Virol.*, **92** (2020), 1995–2003. https://doi.org/10.1002/jmv.25939

16. M. Serhani, H. Labbardi, Mathematical modeling of COVID-19 spreading with asymptomatic infected and interacting peoples, *J. Appl. Math. Comput.*, **66** (2021), 1–20. https://doi.org/10.1007/s12190-020-01421-9

17. X. Huo, J. Chen, S. Ruan, Estimating asymptomatic, undetected and total cases for the COVID-19 outbreak in Wuhan: a mathematical modeling study, *BMC infect. Dis.*, **21** (2021), 1–18. https://doi.org/10.1186/s12879-021-06078-8

18. N. Al-Salti, I. M. Elmojtaba, J. Mesquita, D. Pastore, M. Al-Yahyai, Mathematical Analysis of Diagnosis Rate Effects in Covid-19 Transmission Dynamics with Optimal Control, in *Analysis of Infectious Disease Problems (Covid-19) and Their Global Impact*, Springer, (2021), 219–244. https://doi.org/10.1007/978-981-16-2450-6_11

19. D. Ibarra-Vega, Lockdown, one, two, none, or smart. Modeling containing COVID-19 infection. A conceptual model, *Sci. Total Environ.*, **730** (2020), 138917. https://doi.org/10.1016/j.scitotenv.2020.138917

20. S. Alrashed, N. Min-Allah, A. Saxena, I. Ali, R. Mehmood, Impact of lockdowns on the spread of COVID-19 in Saudi Arabia, *Inform. Med. Unlocked.*, **20** (2020), 100420. https://doi.org/10.1016/j.imu.2020.100420

21. D. Fanelli and F. Piazza, Analysis and forecast of COVID-19 spreading in China, Italy and France, *Chaos Solitons Fractals*, **134** (2020), 109761. https://doi.org/10.1016/j.chaos.2020.109761

22. D. Aldila, S. Khoshnaw, E. Safitri, Y. Anwar, A. Bakry, B. Samiadji, et al., A mathematical study on the spread of COVID-19 considering social distancing and rapid assessment: The case of Jakarta, Indonesia, *Chaos Solitons Fractals*, **139** (2020), 110042. https://doi.org/10.1016/j.chaos.2020.110042

23. N. Ahmad, COVID-19 modeling in Saudi Arabia using the modified Susceptible-Exposed-Infectious-Recovered (SEIR) model, *Cureus*, **12** (2020), e10452. https://doi.org/10.7759/cureus.10452 .

24. S. Ullah, M. A. Khan, Modeling the impact of non-pharmaceutical interventions on the dynamics of novel coronavirus with optimal control analysis with a case study, *Chaos Solitons Fractals*, **139** (2020), 110075. https://doi.org/10.1016/j.chaos.2020.110075

25. S. M. Kassa, J. Njagarah, Y. A. Terefe, Analysis of the mitigation strategies for COVID-19: From mathematical modelling perspective, *Chaos Solitons Fractals*, **138** (2020), 109968. https://doi.org/10.1016/j.chaos.2020.109968

26. Y. Ding, L. Gao, An evaluation of COVID-19 in Italy: A data-driven modeling analysis, *Infectious Disease Modelling*, **5** (2020), 495–501. https://doi.org/10.1016/j.idm.2020.06.007

27. T. Phan, K. Nagaro, Diagnostic Tests for COVID-19, in *Coronavirus Disease-COVID-19*, Springer, (2021), 403–412. https://doi.org/10.1007/978-3-030-63761-3_23

28. A. Khan, H. Alahdal, R. Alotaibi, H. Sonbol, R. Almaghrabi, Y. Alsofayan, et al., Controlling COVID-19 pandemic: A mass screening experience in Saudi Arabia, *Front. Public Health*, **8** (2021), 1013. https://doi.org/10.3389/fpubh.2020.606385

29. Saudi Arabia's Experience in Health Preparedness and Response to COVID-19 Pandemic, 2020. Available from: https://www.moh.gov.sa/en/Ministry/MediaCenter/Publications/Pages/Publications-2020-10-27-001.aspx.

30. Active Surveillance Detects COVID-19 Cases in Makkah and Madinah, 2020. Available from: https://www.moh.gov.sa/en/Ministry/MediaCenter/News/Pages/News-2020-04-18-002.aspx.

31. MOH Announces Third Stage of Expanded COVID-19 Testing, 2020. Available from: https://www.moh.gov.sa/en/Ministry/MediaCenter/News/Pages/News-2020-05-19-006.aspx.

32. MOH: Third Stage of (Takkad) Initiative Centers Launched, 2020. Available from: https://www.moh.gov.sa/en/Ministry/MediaCenter/News/Pages/News-2020-06-17-004.aspx.

33. MOH Performs 200,000 Coronavirus PCR Testing, COVID-19 Monitoring Committee Says, 2020. Available from: https://www.moh.gov.sa/en/Ministry/MediaCenter/News/Pages/News-2020-04-21-005.aspx.

34. Over 600,000 Self-assessment Exams Throught "Mawid" App, COVID-19 Monitoring Committee Says, 2020. Available from: https://www.moh.gov.sa/en/Ministry/MediaCenter/News/Pages/News-2020-04-25-001.aspx.

35. Saudi Arabia Sings 955 Million SR Contract with China for Testing Coronavirus, 2020. Available from: https://www.spa.gov.sa/viewfullstory.php?lang=en&newsid=2079249.

36. MOH: Over 2M Beneficiaries of "Takkad" Centers and "Tetamman" Clinics, 2020. Available from: https://www.moh.gov.sa/en/Ministry/MediaCenter/News/Pages/News-2020-08-12-007.aspx.

37. S. K. Al-Harbi, S. M. Al-Tuwairqi, Modeling the effect of lockdown and social distancing on the spread of COVID-19 in Saudi Arabia, *PLOS ONE*, **17** (2022), 1–40. https://doi.org/10.1371/journal.pone.0265779

38. P. Van Den Driessche, J. Watmough, Reproduction numbers and sub-threshold endemic equilibria for compartmental models of disease transmission, *Math. Biosci.*, **180** (2002), 29–48. https://doi.org/10.1016/S0025-5564(02)00108-6

39. L. Perko, *Differential Equations and Dynamical Systems*, Springer, 2001. https://doi.org/10.1007/978-1-4613-0003-8 .

40. B. E. Meserve, *Fundamental Concepts of Algebra*, Dover Publications, 1982.

41. R. K. Nagle, E. B. Saff, A. D. Snider, *Fundamentals of Differential Equations and Boundary Value Problems*, Pearson/Addison Wesley, 2004.

42. M. Bensoubaya, A. Ferfera, A. Iggidr, Stabilization of nonlinear systems by use of semidefinite Lyapunov functions, *Appl. Math. Lett.*, **12** (1999), 11–17. https://doi.org/10.1016/S0893-9659(99)00095-6

43. J. K. Hale, H. Koçak, *Dynamics and Bifurcations*, Springer, 1991. https://doi.org/10.1007/978-1-4612-4426-4 .

44. General Authority for Statistics Kingdom of Saudi Arabia, 2019. Available from: https://www.stats.gov.sa/en/1007-0.

45. COVID 19 Dashboard: Saudi Arabia, 2020. Available from: https://covid19.moh.gov.sa/.

46. H. Youssef, N. Alghamdi, M. A. Ezzat, A. A. El-Bary, A. M. Shawky, Study on the SEIQR model and applying the epidemiological rates of COVID-19 epidemic spread in Saudi Arabia, *Infect. Dis. Model.*, **6** (2021), 678–692. https://doi.org/10.1016/j.idm.2021.04.005

47. M. Martcheva, *An Introduction to Mathematical Epidemiology*, Springer, 2015. https://doi.org/10.1007/978-1-4899-7612-3

AIMS Press